ČESKÉ VYSOKÉ UČENÍ TECHNICKÉ V PRAZE
Fakulta jaderná a fyzikálně inženýrská
Katedra matematiky

DIPLOMOVÁ PRÁCE

Voronoiova dláždění kvazikrystalů

Voronoi tessellation of quasicrystals

Vypracoval: Eduard Šubert
Školitel: Ing. Petr Ambrož, Ph.D.
Akademický rok: 2016/2017

Na toto místo přijde svázat **zadání diplomové práce**!
V jednom z výtisků musí být **originál** zadání, v ostatních kopie.

prázdná strana pro zadání

Čestné prohlášení

Prohlašuji na tomto místě, že jsem předloženou práci vypracoval samostatně a že jsem uvedl veškerou použitou literaturu.

V Praze dne May 8, 2017 .....

Eduard Šubert

Děkuji Ing. Petrovi Ambrožovi, Ph.D. a prof. Ing. Zuzaně Masákové, Ph.D. za příkladné vedení mé diplomové práce a za podnětné návrhy.

Název práce: **Voronoiova dláždění kvazikrystalů**

Autor: Eduard Šubert

Obor: Matematická informatika

Druh práce: Diplomová práce

Vedoucí práce: Ing. Petr Ambrož Ph.D., Katedra matematiky, FJFI ČVUT v Praze

Abstrakt: Představujeme novou vylepšenou metodu pro hledání všech různých Voronoiových polygonů v kvazikrystalu. Naše vylepšení snižuje nutné teoretické znalosti a v některý případech umožňuje najít i Voronoiovy polygony, které se vyskytují s nulovou hustotou. Naše metoda užívá přesných výpočtů, a tak naše výsledky nejsou přibližné, ale jsou přesné.

Jako je obvyklé i náš model kvazikrystalu užívá schéma Cut-and-project. Nejdříve popisujeme naší metodu obecně, a pak ji aplikujeme na kvazikrystaly s osmi a dvanácti četnou rotační symetrií pro kruhová a osmiúhelníková/dvanáctiúhelníková okna.

Title: **Voronoi tessellation of quasicrystals**

Author: Eduard Šubert

Abstract: A new improved method for finding all distinct Voronoi tiles in any quasicrystal is presented. Our improvement cuts down on necessary theoretical background and in certain cases allows one to find even the Voronoi tiles that appear with zero density. Our method uses precise arithmetic and so our results are not approximations, they are exact.

As per usual our quasicrystal model is based on the Cut-and-project scheme. First we describe our method in general terms and then apply it to two dimensional quasicrystals with 8-fold and 12-fold rotational symmetries for circular and octagonal/dodecagonal windows.

Contents

Introduction

The Nobel Prize in Chemistry 2011 was awarded to Dan Shechtman "for the discovery of quasicrystals" [1]. His discovery opened new areas for research in chemistry, physics as well as in mathematics. We aim to contribute to the growing body of work with our mathematical analysis of several kinds of qusicrystals. Our work is a spiritual successor to series of mathematical articles from 2003 and 2005 [6], [7] and [8] by our colleges that are often referenced by works of physicists ([11], [12], [13], [14]). Therefore we have hopes that our work will also help to better understand this peculiar form of solid matter.

In 1982 Dan Shechtman was studying an alloy of aluminum and manganese with electron microscope. In the diffraction pattern that the electron microscope produced he observed a 10-fold rotational symmetry, that was thought to be impossible. After several years of convincing other scientists of correctness of his observations he succeed. Others remembered that they at some point in their careers observed similar diffraction patterns, but considered them to be mistakes, thus also crystals with 8-fold and 12-fold rotational symmetries in their diffraction patterns were re-discovered. Later a connection was made to previous work of Alan Mackay who used the famous Penrose tessellation to create a theoretical model of matter by placing atoms at vertexes of the Penrose tessellation. He concluded that a diffraction pattern of such model would also have 10-fold rotational symmetry. Thus mathematical analysis of quasicrystals has started, a body of work we now aim to contribute to.

The first chapter contains all the necessary background to study of quasicrystals. Even if you are familiar with these topics we do not recommend skipping the chapter since we define several terms that are not so universal. In Chapter 2 we define what we consider to be a quasicrystal and outline the steps of our general method of analysis. The third chapter is where we do the actual analysis and point to some difficulties where we needed to take extra care. Chapter 4 is the presentation of our results.

Chapter 1

Preliminaries

Definition 1.1. The set $D \subset \mathbb{C}^n$ such that all points are isolated, that is:

$$\forall\, z \in D\ \exists\, \epsilon > 0 :\ B(z, \epsilon) \cap D = \{z\}$$

is a **discrete set**. ⌟

1.1 Delone set

Delone set is such a set that is both relatively dense and uniformly discrete. These notions are defined using two parameters called packing a covering radius.

Definition 1.2. The **packing radius** of a set $D \subset \mathbb{C}^n$ is the number:

$$R_P = \frac{1}{2} \sup \{ r_1 \in \mathbb{R} \mid \forall\, z_1, z_2 \in D, z_1 \neq z_2 :\ \|z_1 - z_2\| > r_1 \}$$

⌟

Remark. Open balls of packing radius centered at the points of the set are disjoint.

Definition 1.3. The **covering radius** of a set $D \subset \mathbb{C}^n$ is the number:

$$R_C = \inf \{ r_2 > 0 \mid \forall\, z \in \mathbb{C}^n :\ B(z, r_2) \cap D \neq \emptyset \}$$

⌟

Remark. Union of closed balls of covering radius centered at the points of the set covers the entire space $\mathbb{C}^n$.

Definition 1.4. Let $D \subset \mathbb{C}^n$.
If D has positive packing radius R_P then it is **uniformly discrete**.
If D has finite covering radius R_C then it is **relatively dense**.
If D has both positive packing radius R_P and finite covering radius R_C then it is a **Delone set**. ⌟

1.2 Voronoi diagram

Voronoi diagram is very useful for analysis of local configurations of discrete sets. Since that is essentially the entirety of our work, we define not only the basic Voronoi polygon but also couple nontraditional terms that will ease our work.

Definition 1.5. Let $P \subset \mathbb{R}^n$ be a discrete set and $x \in P$. The **Voronoi polygon** or **Voronoi cell** or **Voronoi tile** of x on P is the set:

$$V_P(x) = \{y \in \mathbb{R}^n \,|\, \forall z \in P, z \neq x : \|y - x\| \leq \|y - z\|\}$$

Voronoi polygon $V_P(x)$ is said to **belong** to the point x and x is called the **center** of the Voronoi cell $V_P(x)$. ⌟

Remark. When there can be no confusion as to what set P is, the index P may be omitted: $V(x)$.

Definition 1.6. Let $P \subset \mathbb{R}^n$ be a discrete set. The **Voronoi diagram** or **Voronoi tessellation** of P is the set:

$$\{V(x) \,|\, x \in P\}$$

⌟

Definition 1.7. Let $P \subset \mathbb{R}^n$ be a discrete set. The set of centered Voronoi tiles:

$$\{V(x) - x \,|\, x \in P\}$$

is called the **list of Voronoi tiles**. ⌟

Remark. A Voronoi diagram can be viewed as an image whereas a list of Voronoi tiles can be viewed as a list of Voronoi polygon shapes.

Definition 1.8. Let $P \subset \mathbb{R}^n$ be a discrete set and let $x \in P$. The **radius** of Voronoi polygon $V(x)$ is the number:

$$\sup_{y \in V(x)} \|y - x\|$$

⌟

Definition 1.9. Let $P \subset \mathbb{R}^n$ be a discrete set and let $x \in P$. The set of points of P that directly shape the Voronoi polygon $V_P(x)$:

$$D_P(x) = \bigcap \left\{Q \subset P \,|\, V_Q(x) = V_P(x)\right\}$$

is called the **domain** of x or of $V_P(x)$. ⌟

It will be very useful to explore the Voronoi tessellation on a Delone set.

Theorem 1.10. *Let $P \subset \mathbb{R}^n$ be a Delone set with covering radius R_C and let $x \in P$. Then*

$$V(x) \subset \overline{B(x, R_C)}$$

Proof. By definition of the covering radius (1.3), for any point $y \in \mathbb{R}^n \setminus \overline{B(x, R_C)}$ there exists $w \in P$ such that $w \in B(y, R_C)$. Therefore w is closer to y than x and so $y \notin V(x)$. □

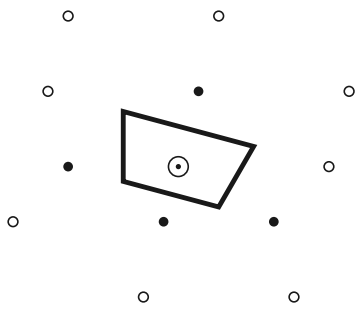

Figure 1.1: Example of a Voronoi tile. The set P consists of all the points $\bullet$, $\circ$ and $\odot$. The polygon is the Voronoi cell belonging to the $\odot$ point. The $\bullet$ points are the domain of the Voronoi polygon (i.e. the $\circ$ points do not affect the shape of the Voronoi polygon).

Theorem 1.11. *Let $P \subset \mathbb{R}^n$ be a Delone set with covering radius R_C and let $x \in P$. Then*

$$D(x) \subset B(x, 2R_C)$$

Proof. For $y \in P$ such that $\|y - x\| \geq 2R_C$ there exists a point $z \in \mathbb{R}^n$ such that $\|y - z\| \geq \|x - z\| \geq R_C$. Thus if y were in $D(x)$ the Voronoi tile would not be inside $\overline{B(x, R_C)}$. □

The relationship between a Voronoi polygons and the covering radius is actually even more intricate, as the following theorem shows.

Theorem 1.12. *Let $P \subset \mathbb{R}^n$ be a Delone set with covering radius R_C and let $x \in P$. Then the covering radius R_C is the supremum of the radii of the Voronoi tiles:*

$$R_C = \sup_{x \in P} \left\{ \sup_{y \in V(x)} \|y - x\| \right\}$$

Proof. Let us denote the supremum of radii $r = \sup_{x \in P} \left\{ \sup_{y \in V(x)} \|y - x\| \right\}$. We have already proved that $r \leq R_C$. Now assume that $r < R_C$. Then there is a point $y \in \mathbb{R}^n$ such that $B(y, R_C) \cap P = \emptyset$ and yet $y \in V(w)$ for some $w \in P$ and thus $\|w - y\| \leq r$. That is of course a contradiction. □

1.3 Number theory

The study of quasicrystals relies heavily on number theory. Therefore this section lists definitions and their corollaries that are used further. For proofs of our claims we refer the reader to [4].

Definition 1.13. Let $P \subset \mathbb{C}$. The ring of polynomials in x with coefficients in P is denoted by $P[x]$. ⌟

Definition 1.14. Polynomial $f \in \mathbb{C}[x]$ such that $f(x) = \sum_{k=0}^{m} \alpha_k x^k$ for some $m \in \mathbb{N}$, where $\alpha_m = 1$ is a **monic polynomial**. ⌟

Definition 1.15. Polynomial $f \in \mathbb{C}[x]$ such that $\forall\, g, h \in \mathbb{C}[x] : \ f \neq gh$ is an **irreducible polynomial**. ⌟

1.3.1 Algebraic numbers, minimal polynomial and degree

Definition 1.16. Let $\alpha, \beta \in \mathbb{C}$.
If there exists a monic polynomial $f \in \mathbb{Q}[x]$ such that $f(\alpha) = 0$, then α is an **algebraic number**. The set of algebraic numbers is denoted as $\mathbb{A}$.
If there exists a monic polynomial $g \in \mathbb{Z}[x]$ such that $g(\beta) = 0$, then β is an **algebraic integer**. The set of algebraic integers is denoted as $\mathbb{B}$. ⌟

Definition 1.17. Irreducible monic polynomial $f \in \mathbb{Q}[x]$ of the smallest degree such that $f(\alpha) = 0$ for $\alpha \in \mathbb{A}$ is the **minimal polynomial** of α. It is usually denoted as f_α. ⌟

Definition 1.18. The **degree** of an algebraic number is the degree of its minimal polynomial. ⌟

Remark. For each algebraic number there exists exactly one minimal polynomial.

1.3.2 Galois isomorphism

Definition 1.19. Let $\alpha \in \mathbb{A}$ of degree m and $f_\alpha \in \mathbb{Q}[x]$ be its minimal polynomial. The $(m-1)$ other roots of f_α are called **conjugate roots** of α and are denoted as $\alpha^{(1)}$, $\alpha^{(2)}$, …, $\alpha^{(m-1)}$. ⌟

Remark. Consistently with the notation of its conjugate roots, α may be denoted as $\alpha^{(0)}$ or $\alpha^{(m)}$.

Remark. For low degrees the upper indexes are often written in unary – e.g. $\alpha, \alpha', \alpha''$.

Definition 1.20. Let $\alpha \in \mathbb{A}$ of degree m. The **extension ring** of the number α is the set:

$$\mathbb{Z}(\alpha) = \left\{ a_0 + a_1\alpha + a_2\alpha^2 + \cdots + a_{m-1}\alpha^{m-1} \mid a_i \in \mathbb{Z} \right\}$$

⌟

Definition 1.21. Let $\alpha \in \mathbb{A}$ of degree m. The **extension field** of the number α is the set:

$$\mathbb{Q}(\alpha) = \left\{ b_0 + b_1\alpha + b_2\alpha^2 + \cdots + b_{m-1}\alpha^{m-1} \mid b_i \in \mathbb{Q} \right\}$$

⌟

Remark. Extension ring of α is the smallest ring containing α as well as all integers. Extension field of α is the smallest field containing α as well as all rationals.

Definition 1.22. Let $\alpha \in \mathbb{A}$ of degree m and let $\alpha^{(1)}$, $\alpha^{(2)}$, …, $\alpha^{(m-1)}$ be its conjugate roots. Then $\mathbb{Q}(\alpha)$, $\mathbb{Q}(\alpha')$, …, $\mathbb{Q}(\alpha^{(m-1)})$ are isomorphic. The **Galois isomorphisms** are:

$$\sigma_i : \mathbb{Q}(\alpha) \to \mathbb{Q}\big(\alpha^{(i)}\big) \quad \text{induced by} \quad \sigma_i(\alpha) = \alpha^{(i)} \qquad i \in \widehat{m-1}$$

⌟

Galois isomorphisms play a significant role in the definition of the quasicrystals, so they surely deserve an example.

The Galois isomorphism σ_0 is always identity.

In general the Galois isomorphism σ_i exchanges α of degree m with its ith conjugate root.

$$\sigma_i\big(b_0 + b_1\alpha + b_2\alpha^2 + \cdots + b_{m-1}\alpha^{m-1}\big) = b_0 + b_1\alpha^{(i)} + b_2\big(\alpha^{(i)}\big)^2 + \cdots + b_{m-1}\big(\alpha^{(i)}\big)^{m-1}$$

Since further we will only work with quadratic algebraic numbers (i.e. of degree 2), there will only be two roots of a given minimal polynomial, α and α', and two Galois isomorphisms, namely the identity and $\sigma_1(\alpha) = \alpha'$. Moreover, $\alpha' \in \mathbb{Q}(\alpha)$, thus σ_1 is an automorphism of the quadratic field $\mathbb{Q}(\alpha)$ and is often denoted only as $'$ – i.e. $\sigma_1(x) = x'$ for $x \in \mathbb{Q}(\alpha)$.

1.3.3 Root of unity, cyclotomic polynomial

Definition 1.23. Every $\zeta \in \mathbb{C}$ such that $\zeta^n - 1 = 0$ for $n \in \mathbb{N}$ is called the n**th root of unity** or just **root of unity** if n is not given. Minimal $d \in \mathbb{N}$ for which $\zeta^d - 1 = 0$ is the **order** of ζ. Nontrivial root of unity is different from one. ⌟

Remark. Nontrivial root of unity is a root of polynomial $\frac{x^n-1}{x-1}$.

Remark. nth root of unity may be written as $\zeta = e^{2k\pi \mathrm{i}/n}$ for $k \in \{0, 1, \ldots, n-1\}$.

Theorem 1.24. *Degree of nth root of unity ζ is $\varphi(n)$, where φ is the Euler function.*

Now we would like to look at the Galois isomorphisms of nth root of unity ζ of degree 4. It will be evident why 4 later. By previous theorem, that means $\varphi(n) = 4$.

The three conjugate roots of ζ are also nth roots of unity and as such they are powers of ζ, specifically $\{\zeta^k \mid k \perp n, k > 1\}$.

Since $k \perp n$ implies $(n-k) \perp n$ and also

$$\cos\left(\frac{2k\pi}{n}\right) = \cos\left(\frac{2\,(n-k)\,\pi}{n}\right) \quad \text{and} \quad \sin\left(\frac{2k\pi}{n}\right) = -\sin\left(\frac{2\,(n-k)\,\pi}{n}\right)$$

the four roots $\zeta^{(0)}, \zeta^{(1)}, \zeta^{(2)}, \zeta^{(3)}$ appear in pairs of complex conjugates. Therefore among the four Galois isomorphisms there are two that do not change the real part of ζ and two that do change it. This will become very significant once we introduce the Pisot-cyclotomic numbers.

1.3.4 Pisot numbers

Definition 1.25. Let $\beta \in \mathbb{B}$ be an algebraic integer of degree m, $\beta > 1$ and for all conjugate roots β', β'', …, $\beta^{(m-1)}$ it holds

$$|\beta^{(i)}| < 1 \qquad \forall\, i \in \widehat{m-1}$$

Then β is called **Pisot** number. ⌟

As we will see in Section 2.2, Pisot numbers represent another crucial notion to our quasicrystal model.

1.3.5 Vieta's formulas

Since we will work a lot with roots of quadratic equations we want to, just for completeness, show the Vieta's formulas in the form in which we will use them.

The roots $x, x' \in \mathbb{C}$ of quadratic polynomial $ax^2 + bx + c$ satisfy:

$$x + x' = -\frac{b}{a} \qquad \text{and} \qquad xx' = \frac{c}{a}$$

For a monic quadratic polynomial ($a = 1$) we have:

$$x + x' = -b \qquad \text{and} \qquad xx' = c$$

We will often want to express one root in terms of the other:

$$x = -b - x' \qquad \text{and} \qquad x = \frac{c}{x'}$$

1.4 Crystallography

Even though we are further going to work only with quasicrystals, they are often described by their differences from crystals. Therefore we briefly touch on the very basics of crystallography.

A lattice is usually used as a model for a crystal.

Definition 1.26. Let $\{\mathbf{e}_1, \ldots, \mathbf{e}_d\}$ be a basis of $\mathbb{R}^d$ for $d \in \mathbb{N}$. **Lattice** in $\mathbb{R}^d$ is the set

$$L = \bigoplus_{j=1}^{d} \mathbb{Z}\,\mathbf{e}_j$$

⌟

There is an important theorem in crystallography, the crystallographic restriction theorem [2], that limits the rotational symmetries available to crystals. Here we only show the two dimensional variant.

Theorem 1.27. *Two dimensional lattices are limited to 2-fold, 3-fold, 4-fold, and 6-fold rotational symmetries.*

These rotational symmetries, 2-fold, 3-fold, 4-fold, and 6-fold, are thus called **crystallographic** rotational symmetries.

Quasicrystals are of course not bounded by the crystallographic restriction theorem and therefore have different rotational symmetries, we will call these different rotational symmetries **non-crystallographic**.

1.5 Cut-and-project scheme

We are using cut-and-project scheme to model the quasicrystals. Here is a brief introduction into its workings. In general, cut-and-project is a specific way of selecting a subset from a larger set.

The cut-and-project scheme utilizes $m + n$ dimensional lattice $L \subset \mathbb{R}^{m+n}$, m dimensional subspace $V_1 \subset \mathbb{R}^{m+n}$ and n dimensional subspace $V_2 \subset \mathbb{R}^{m+n}$. Further we define two projections $\pi_1 : \mathbb{R}^{m+n} \to V_1$ and $\pi_2 : \mathbb{R}^{m+n} \to V_2$ such that $\pi_1|_L$ is injection and $\pi_2(L)$ is dense in V_2.

These projections are where the 'project' part of the cut-and-project scheme comes from. The 'cut' part comes from a bounded subset $\Omega \subset V_2$ with nonempty interior usually referred to as **window**.

All put together the cut-and-project scheme produces a subset $Q \subset \pi_1(L)$:

$$Q = \{\pi_1(x) \mid \pi_2(x) \in \Omega,\, x \in L\}$$

Put in words the set Q are π_1 projections of those points of L whose π_2 projections fit in the window Ω.

The notation can be somewhat simplified by composing a projection between $\pi_1(L)$ and $\pi_2(L)$: $\pi_2 \circ \pi_1^{-1}$, usually denoted as $*$ and referred to as the **star map**. Q then becomes:

$$Q = \{x \in V_1 \mid x^* \in \Omega\}$$

This is the form in which we will use the cut-and-project scheme.

Chapter 2

Quasicrystal

2.1 Quasicrystal

Unfortunately, there is so far no established mathematical definition of a quasicrystal, in the most basic terms it is just a set that is ordered but not periodic.

We are going to introduce our own attributes that a set $\Lambda \subset \mathbb{C}$ needs to have to be a quasicrystal.

First we require Λ to be not too dense but also not too discrete. In other words to have uniform discreetness as well as finite density.

1. uniform discreteness:
$$\exists\, r_1 > 0,\ \forall z_1, z_2 \in \Lambda, z_1 \neq z_2 :\ |z_1 - z_2| > r_1$$
2. relative density:
$$\exists\, r_2 > 0,\ \forall z \in \mathbb{C} :\ B(z, r_2) \cap \Lambda \neq \emptyset$$

Next we want finite local complexity. Sometimes this attribute is written as finiteness of the set of intersections of Λ with balls of fixed but arbitrary radius centered at any point of Λ:

$$\forall\, \rho > 0 :\ \big|\{\Lambda \cap B(x, \rho) \mid \forall x \in \Lambda\}\big| < \infty$$

However since we are going to study the Voronoi diagram of Λ we directly require the list of Voronoi tiles of Λ to be finite.

3. finite local complexity:
$$\big|\{V(x) - x \,|\, x \in \Lambda\}\big| < \infty$$

So far we have achieved the orderedness part but even periodic lattices have these properties. To break the periodicity we are going to require non-crystallographic rotational symmetry and nontrivial dilation.

4. rotational symmetry:
$$\exists\, \zeta = e^{2\pi \mathrm{i}/n},\ n \in \mathbb{N} \setminus \{2, 3, 4, 6\} :\ \zeta\Lambda = \Lambda$$

5. dilation:

$$\exists\, \beta \in \mathbb{R} \setminus \{-1, 1\} : \ \beta\Lambda \subset \Lambda$$

It stems form these properties alone, that among other constants a quasicrystal is linked to a root of unity ζ and to a number $\beta \in \mathbb{R} \setminus \{-1, 1\}$. Of course not every pair (ζ, β) is associated with a quasicrystal.

In the next section we will go through parameters ζ and β which are associated with a quasicrystal and we will explain where do they come from.

2.2 Pisot-cyclotomic numbers

Pisot-cyclotomic numbers are Pisot numbers and are algebraically related to roots of unity. We will use these numbers in place of β from previous section.

Definition 2.1. Let $\rho = 2\cos(2\pi/n)$ for a given $n > 4$, its extension ring $\mathbb{Z}[\rho]$ and m order of ρ. A **Pisot-cyclotomic** number of degree m, of order n associated to ρ is a Pisot number $\beta \in \mathbb{Z}[\rho]$ such that

$$\mathbb{Z}[\beta] = \mathbb{Z}[\rho]$$

⌟

Nontrivial nth root of unity $\zeta = e^{2\pi \mathrm{i}/n}$ is by definition a solution to equation

$$\frac{\zeta^n - 1}{\zeta - 1} = \zeta^{n-1} + \zeta^{n-2} + \cdots + \zeta + 1 = 0$$

further for $\rho = 2\cos(2\pi/n)$ it holds

$$\rho = \zeta + \bar{\zeta} \quad \Rightarrow \quad \zeta^2 = \rho\zeta - 1$$

Therefore for extension rings $\mathbb{Z}[\zeta]$ and $\mathbb{Z}[\rho]$ we have

$$\mathbb{Z}[\zeta] = \mathbb{Z}[\rho] + \mathbb{Z}[\rho]\,\zeta$$

and finally for Pisot-cyclotomic β associated to ρ we acquire

$$\mathbb{Z}[\zeta] = \mathbb{Z}[\beta] + \mathbb{Z}[\beta]\,\zeta$$

Such countable ring is of course n-fold rotationally invariant

$$\zeta^k \mathbb{Z}[\zeta] \subset \mathbb{Z}[\zeta] \qquad k \in \widehat{n-1}$$

To summarize β is Pisot (and thus real) and it can be used to decompose n-fold rotationally invariant complex ring $\mathbb{Z}[\zeta]$ as $\mathbb{Z}[\beta] + \mathbb{Z}[\beta]\,\zeta$.

For further work we will need actual values of Pisot-cyclotomic numbers and so in the next section we will show a method for finding quadratic Pisot-cyclotomic numbers, whose quasicrystals we will later analyze. The method could of course be generalized to different degrees.

2.2.1 Quadratic Pisot-cyclotomic numbers

Remark. Even though we are mainly focusing on two dimensional quasicrystals, that is not dictated by the quadratic-ness of β. Quadratic Pisot-cyclotomic numbers are also associated to quasicrystals of arbitrary dimension.

As stated in preliminaries, the degree of root of unity of order n is $\varphi(n)$ (where φ is the Euler function). From the decomposition in the previous section we can easily infer that the degree of ζ is double of degree of β (or ρ). Moreover, we are looking for β of degree 2. Together we acquire the following equation.

$$\varphi(n) = 2 \cdot 2 = 4$$

With help from the Euler product formula we can show that such equation holds only for $n \in \{5, 8, 10, 12\}$.

For each $n \in \{5, 8, 10, 12\}$ there is $\rho = 2\cos(2\pi/n)$ and for each such ρ there are $\beta \in \mathbb{Z}[\rho]$ following Definition 2.1. Each of these numbers β is associated to the same quasicrystal and so it is sufficient to pick only one representative.

Moreover, since $2\cos(2\pi/5) = \frac{\sqrt{5}-1}{2} = \frac{\sqrt{5}+1}{2} - 1 = 2\cos(2\pi/10) - 1$ the extension rings $\mathbb{Z}[2\cos(2\pi/5)]$ and $\mathbb{Z}[2\cos(2\pi/10)]$ are identical and by extension the quasicrystals associated are also the same. Therefore we can skip the 5-fold rotational symmetry.

To summarize, quadratic Pisot-cyclotomic numbers β can only be associated to quasicrystals with 8-fold, 10-fold or 12-fold rotational symmetries. Table 2.1 shows a list of quadratic Pisot-cyclotomic numbers interesting for Quasicrystallography.

n	ρ	β	ζ
8	$2\cos\left(\frac{2\pi}{8}\right)$	$1+\sqrt{2}$	$e^{2i\pi/8}$
10	$2\cos\left(\frac{2\pi}{10}\right)$	$\frac{1+\sqrt{5}}{2}$	$e^{2i\pi/10}$
12	$2\cos\left(\frac{2\pi}{12}\right)$	$2+\sqrt{3}$	$e^{2i\pi/12}$

Table 2.1: Pisot-cyclotomic numbers of degree 2, of order n, associated to ρ.

Now we want to explore the connection between Galois isomorphisms of ζ and β. As we have shown here and in Section 1.3.3, for quadratic Pisot-cyclotomic β the associated root of unity ζ is of degree 4 and among its four Galois isomorphisms there are two that do not change the real part of ζ. Consequently they also do not alter $\rho = \zeta + \bar{\zeta} = 2\Re(\zeta)$ and by extension neither they alter ρ's extension ring $\mathbb{Z}[\rho]$. By further extension these two Galois isomorphisms of ζ also do not change $\beta \in \mathbb{Z}[\beta] = \mathbb{Z}[\rho]$.

It turns out that the other two Galois isomorphisms of ζ do change β to its conjugate root β', these two are important for our model of the quasicrystal, which we will present in the next section.

2.3 Quasicrystal model

There certainly are many ways to acquire a set that follows the attributes listed in Section 2.1. We utilize the cut-and-project scheme described in Section 1.5.

Even though we showed the two dimensional quasicrystal as a subset of $\mathbb{C}$ it is sometimes preferable to treat it as a subset of $\mathbb{R}^2$. Thus we present two definitions of our model of a quasicrystal, one in $\mathbb{C}$ (Definition 2.2) and one in $\mathbb{R}^2$ (Definition 2.3).

Definition 2.2. Let $n \in \mathbb{N} \setminus \{2, 3, 4, 6\}$. Let β be a quadratic Pisot-cyclotomic number of order n, associated to $\rho = 2\cos(2\pi/n)$ (and $\zeta = e^{2\pi \mathrm{i}/n}$). Further, let $*^{\mathbb{C}}$ be a Galois isomorphism of ζ, such that $\beta^{*^{\mathbb{C}}} = \beta'$. Let $M^{\mathbb{C}} = \mathbb{Z}[\beta] + \mathbb{Z}[\beta]\,\zeta$ and $N^{\mathbb{C}} = \mathbb{Z}\left[\zeta^{*^{\mathbb{C}}}\right]$. Lastly, let $\Omega^{\mathbb{C}} \subset N^{\mathbb{C}}$ be bounded with nonempty interior. The **complex model of two dimensional quasicrystal linked to irrationality β and window $\Omega^{\mathbb{C}}$** is the set:

$$\Sigma(\Omega^{\mathbb{C}}) = \{x \in M^{\mathbb{C}} \mid x^{*^{\mathbb{C}}} \in \Omega^{\mathbb{C}}\}$$

⌟

Following Definition 2.3 uses objects defined in Definition 2.2.

Definition 2.3. Let $n \in \mathbb{N} \setminus \{2, 3, 4, 6\}$. Let β be a quadratic Pisot-cyclotomic number of order n, associated to $\rho = 2\cos(2\pi/n)$ (and $\zeta = e^{2\pi \mathrm{i}/n}$). Further, let $* : \mathbb{R}^2 \to \mathbb{R}^2$ be defined as $(x, y)^* = (\Re\big((x + iy)^{*^{\mathbb{C}}}\big), \Im\big((x + iy)^{*^{\mathbb{C}}}\big))$. Let $v_1, v_2 \in \mathbb{R}^2$:

$$v_1 = (1, 0) \quad \text{and} \quad v_2 = (\Re(\zeta), \Im(\zeta))$$

Let $M = \mathbb{Z}[\beta]\,v_1 + \mathbb{Z}[\beta]\,v_2$ and similarly let $N = \mathbb{Z}[\beta]\,v_1^* + \mathbb{Z}[\beta]\,v_2^*$. Lastly, let $\Omega \subset N$ be bounded with nonempty interior. The **model of two dimensional quasicrystal linked to irrationality β and window Ω** is the set:

$$\Sigma(\Omega) = \{x \in M \mid x^* \in \Omega\}$$

⌟

So far the entire theses was purely abstract. To illustrate what a quasicrystal might look like, there is Figure 2.1 which shows finite section of a two dimensional quasicrystal with 8-fold rotational symmetry.

To validate our quasicrystal model we of course have to show that it follows the attributes from Section 2.1. However first we list few properties of our model which will help us show the validity of our model.

- Inclusion property:
$$\Omega_1 \subset \Omega_2 \quad \Rightarrow \quad \Sigma(\Omega_1) \subset \Sigma(\Omega_2)$$
- Union property:
$$\Sigma(\Omega_1 \cup \Omega_2) \;=\; \Sigma(\Omega_1) \cup \Sigma(\Omega_2)$$
- Translation property:
$$\Sigma(\Omega + x^*) \;=\; \Sigma(\Omega) + x \qquad \text{for } x \in M$$
- Scaling property:
$$\Sigma(\beta\Omega) \;=\; \beta'\Sigma(\Omega)$$

And now to validate our model.

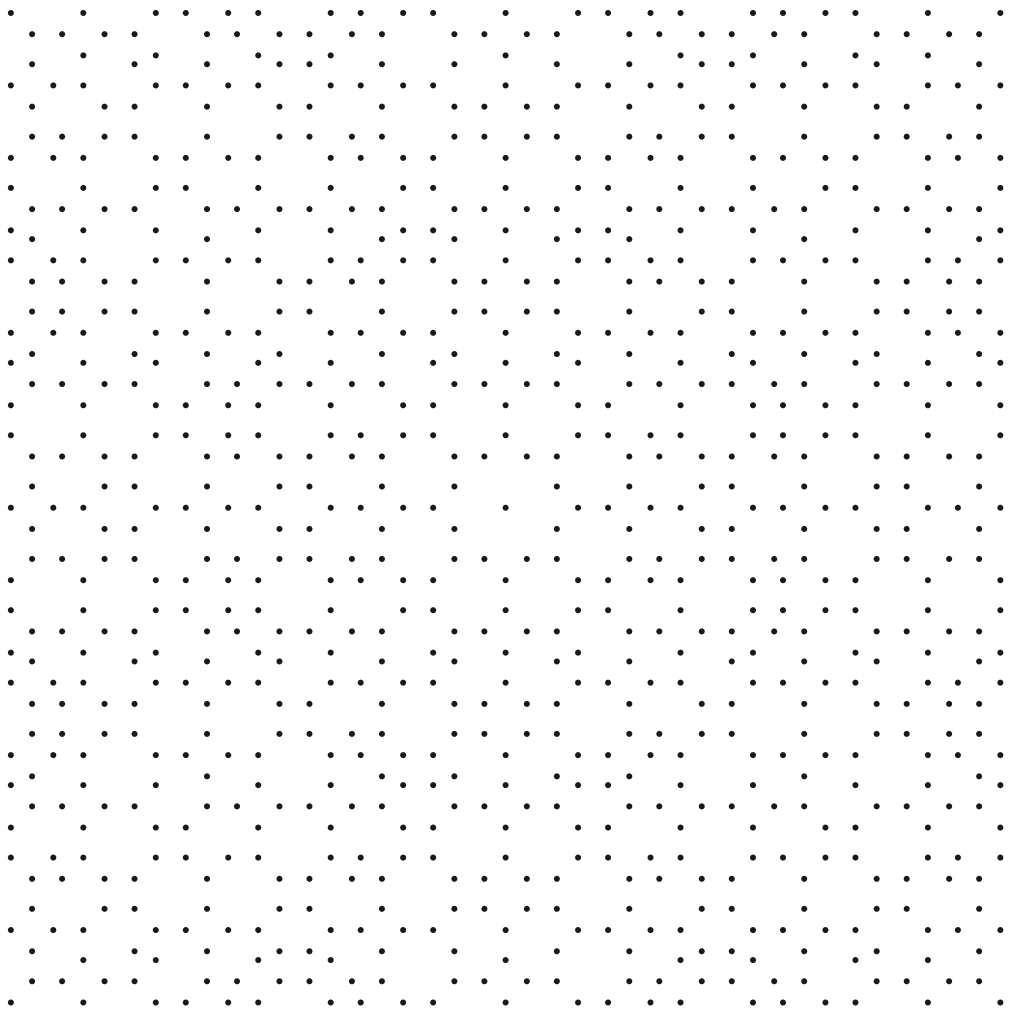

Figure 2.1: Example of a two dimensional quasicrystal.

1. uniform discreteness:

$$\exists\, r_1 > 0,\ \forall z_1, z_2 \in \Lambda, z_1 \neq z_2 :\ |z_1 - z_2| > r_1$$

2. relative density:

$$\exists\, r_2 > 0,\ \forall z \in \mathbb{C} :\ B(z, r_2) \cap \Lambda \neq \emptyset$$

   The result of the cut-and-project scheme is a Delone set [3] if the window Ω is bounded with nonempty interior, which is how we defined it.

3. finite local complexity:

$$\left|\{V(x) - x \,|\, x \in \Lambda\}\right| < \infty$$

   It has been shown [3] that our model has even this property, however since our work explores the list of Voronoi tiles we essentially prove this in the process.

4. rotational symmetry:
$$\exists\, \zeta = e^{2\pi \mathrm{i}/n} :\ \zeta\Lambda^{\mathbb{C}} = \Lambda^{\mathbb{C}}$$
Rotational symmetry appears in quasicrystal if the window Ω has the same rotational symmetry.

5. dilation:
$$\exists\, b \in \mathbb{R} \setminus \{-1, 1\} :\ b\Lambda \subset \Lambda$$
Using the scaling property and the inclusion property:
$$\beta\Sigma(\Omega) = \Sigma(\beta'\Omega) \subset \Sigma(\Omega)$$

Having quasicrystal defined and our model validated, we shall present our plan for the analysis.

2.4 General quasicrystal analysis

In this section we will outline a general method of analysis of any quasicrystal. Later we will use this method to analyze two dimensional quasicrystals.

Analysis should reveal the structure of the points of the quasicrystal, for us that means acquiring the list of Voronoi tiles for each quasicrystal.

To acquire such list we follow these steps:

1. **Acquire arbitrary finite section of the quasicrystal**
   In other words this means creating an algorithm that for a finite section $P \subset \mathbb{R}^d$ returns $P \cap \Sigma(\Omega)$.

2. **Estimate the covering radius R_C of the quasicrystal**
   We are specifically interested in the upper bound $\hat{R}_C$ of the covering radius. This is necessary since in a Delone set Voronoi tile's domain's points can be no further from the center then double of the covering radius.

3. **Generate a superset of all finite sections spanning $B(2\hat{R}_C)$**
   Each of these finite sections represents one Voronoi tile that appears in the quasicrystal's voronoi diagram.

4. **Filter the superset to the final list of Voronoi tiles**
   Due to technical constrains previous step may have created more tiles than there actually are in the list of Voronoi tiles and so it needs to be filtered.

There is also a sort of a fifth step of the analysis that is no longer fixed on a single window of certain size, but explores the changes in the quasicrystal with changing window size.

5. **Establish the period of each Voronoi tile**
   A Voronoi tile generally appears in quasicrystals for whole interval of window sizes. Goal of this step is to establish the endpoints of such interval.

These steps are general enough to analyze any quasicrystal linked to any Pisot-cyclotomic number and in any dimension. Unfortunately, they are also too general and we will need to specify them for each specific quasicrystal.

We close this chapter and our general overview of quasicrystals with discussion of window shapes. It is obviously impossible to analyze a quasicrystal for arbitrary bounded $\Omega \subset N$ with nonempty interior. That is however not necessary. Not every two windows generate different quasicrystals, especially since we do not consider translated and/or β inflated quasicrystals to be different.

2.4.1 Analyzed window shapes

We will use the properties of quasicrystals to gradually limit the set of analyzed windows. We start with all of the windows:

$$\{\Omega \,|\, \Omega \subset N, \text{ bounded with nonempty interior}\}$$

To maintain our sanity we first limit our scope to convex bounded windows with nonempty interior.

$$\{\Omega \,|\, \Omega \subset N, \text{ convex bounded with nonempty interior}\}$$

Further thanks to the translation property we can limit our scope to convex bounded windows with nonempty interior centered around the origin:

$$\{\Omega - C_\Omega \,|\, \Omega \subset N, \text{ convex bounded with nonempty interior}\}$$

where C_Ω is the centroid or geometric center of the window Ω.

Lastly thanks to the scaling property we can limit our scope to convex bounded windows with nonempty interior centered around the origin of diameter in $(1, \beta]$:

$$\{\Omega - C_\Omega, \,|\, \Omega \subset N, \ d(\Omega) \in (1, \beta], \text{ convex bounded with nonempty interior}\}$$

where $d(\Omega)$ is the set diameter $d(\Omega) = \sup\{d(x, y) \,|\, x, y \in \Omega\}$, where $d(x, y)$ is the distance between x and y.

Remark. We could of course also pick any other β multiple of $(1, \beta]$.

Of course even after all this limiting, the set of windows is still infinite. Therefore we will further limit our scope to three basic window shapes: rhombus, regular n-gon and a circle. The rhombus is not really a valid window since it is not sufficiently rotationally symmetrical, it is however fundamental to our method, more on this later. The regular n-gon represents the simplest window with sufficient rotational symmetry and the circle is interesting for its circular symmetry.

To summarize we will analyze quasicrystals for windows in shape of rhombus, regular n-gon and a circle centered around the origin of diameter in $(1, \beta]$. Technically there is an infinite amount of these windows as well however as we will see later it is already manageable.

Finally we need to discuss the boundaries of the windows. Generally we will assume closed windows i.e. we will include the boundary. The exception is the rhombus for reasons we will also explain later.

Now we have quasicrystal defined, model explored and windows limited. In the next chapter we will finally start the analysis.

Chapter 3

Analysis

The first step of analysis of a two dimensional quasicrystal is to create an algorithm for acquiring arbitrary finite section of the quasicrystal. That is however not so simple. Luckily there is a workaround. Using specific window shape it is possible to decompose two dimensional quasicrystal into two quasicrystals with one dimensional windows. We will explain exactly what that means later, for now let us explore two dimensional quasicrystals with one dimensional windows.

By definition a quasicrystal with one dimensional window is a set of points whose star map images fit into a bounded section of a line. Since the star map inverse image of a line is again a line then two dimensional quasicrystal with a line segment for a window is in fact one dimensional (i.e. set of points on a line).

We present this connection between two dimensional and one dimensional quasicrystal mainly to avoid the need to explicitly define the attributes and to show the properties of one dimensional quasicrystals. This way aside from the rotational symmetry all the attributes and all the properties apply to the one dimensional quasicrystal as well.

To summarize: the motivation behind the analysis of one dimensional quasicrystal is the eventual analysis of two dimensional quasicrystal. To take full advantage of previous work we view one dimensional quasicrystal as a special case of two dimensional quasicrystal, that is two dimensional quasicrystal with a line segment for a window.

3.1 One dimensional quasicrystal

We can simplify our model for the specific case of one dimensional window. The easiest way is to position the window along the line $\{(x, 0)|x \in \mathbb{R}\}$. That will result in a quasicrystal along the same line and thus we arrive to the following special case of the model of two dimensional quasicrystal:

Let β be a quadratic Pisot-cyclotomic number of order n, associated to $\rho = 2\cos(2\pi/n)$. Further, let $M = \mathbb{Z}[\beta]$ be the extension ring of β and $N = \mathbb{Z}[\beta']$ the extension ring of β's conjugate root. The projection $* : M \to N$ is the Galois isomorphism σ_1 (often denoted as $'$). Lastly, let $\Omega \subset N$ be bounded with nonempty interior.

Then the **model of one dimensional quasicrystal linked to irrationality β and win-**

dow Ω is the set:

$$\Sigma(\Omega) = \{x \in M \mid x^* \in \Omega\} = \left\{x \in \mathbb{Z}[\beta] \mid x' \in \Omega\right\}$$

Convex bounded one dimensional window is a line segment, which is in one dimension represented by an interval, specifically we will use left-closed right-open interval $\Omega = \left[-\frac{\ell}{2}, \frac{\ell}{2}\right)$ where $\ell \in (1, \beta]$.

As we see in the following breakdown, quasicrystals with different openness or closeness of the window differ only by at most a single point.

$$\Sigma((c,d)) = \begin{cases} \Sigma([c,d)) & c \notin \mathbb{Z}[\beta] \\ \Sigma([c,d)) \setminus \{c'\} & c \in \mathbb{Z}[\beta] \end{cases}$$

$$\Sigma([c,d]) = \begin{cases} \Sigma([c,d)) & d \notin \mathbb{Z}[\beta] \\ \Sigma([c,d)) \cup \{d'\} & d \in \mathbb{Z}[\beta] \end{cases}$$

$$\Sigma((c,d]) = \begin{cases} \Sigma((c,d)) & d \notin \mathbb{Z}[\beta] \\ \Sigma((c,d)) \cup \{d'\} & d \in \mathbb{Z}[\beta] \end{cases}$$

Unfortunately the addition or the removal of a single point causes occurrences of local configurations that appear only once in the entire quasicrystal. That would needlessly complicate our work and therefore we chose to only analyze left-closed right-open interval, which does not suffer from these zero density occurrences.

According to our plan, the first step of the analysis is generating arbitrary finite section of one dimensional quasicrystal.

3.1.1 Arbitrary finite section

Figure 3.1 illustrates well, what we want to acquire – the sequence of points on the M axis. For this purpose we define the sequence of the quasicrystal.

Definition 3.1. Strictly increasing sequence $(y_n^\Omega)_{n\in\mathbb{Z}}$ defined as $\left\{y_n^\Omega \mid n \in \mathbb{Z}\right\} = \Sigma(\Omega)$ where $\Sigma(\Omega)$ is one dimensional quasicrystal is called the **sequence of the quasicrystal** $\Sigma(\Omega)$. ⌟

Now we would like to explore the set of all possible distances between two consecutive points of the sequence of the quasicrystal:

$$\left\{y_{n+1}^\Omega - y_n^\Omega \mid n \in \mathbb{N}\right\}$$

For that we need an expression for y_n^Ω. Let us start with the simplest window: $[-\frac{1}{2}, \frac{1}{2})$. The key here is the length of the window – i.e. 1. First we do a little algebraic exercise with the

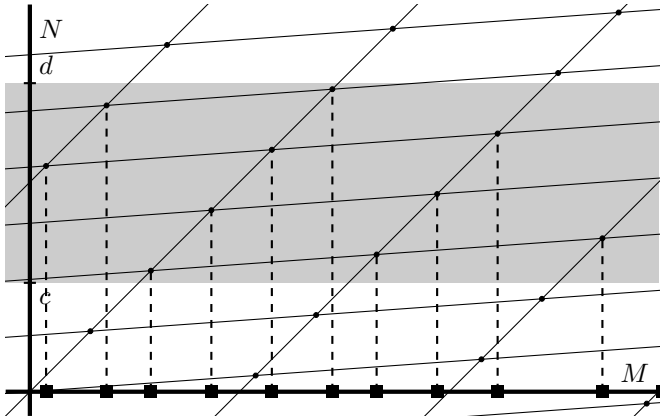

Figure 3.1: Illustration of one-dimensional quasicrystal. The grid is $M \times N$. On the N axis there is a window $\Omega = [c, d)$. The squares on the M axis are points of the quasicrystal $\Sigma(\Omega)$.

expression for the quasicrystal:

$$\begin{aligned}
\Sigma\left(\left[-\frac{1}{2}, \frac{1}{2}\right)\right) &= \left\{ x \in \mathbb{Z}\left[\beta\right] \;\middle|\; x' \in \left[-\frac{1}{2}, \frac{1}{2}\right) \right\} \\
&= \left\{ a + b\beta \;\middle|\; a + b\beta' \in \left[-\frac{1}{2}, \frac{1}{2}\right),\, a, b \in \mathbb{Z} \right\} \\
&= \left\{ a + b\beta \;\middle|\; -\frac{1}{2} \leq a + b\beta' < \frac{1}{2},\, a, b \in \mathbb{Z} \right\} \\
&= \left\{ a + b\beta \;\middle|\; -\frac{1}{2} - b\beta' \leq a < \frac{1}{2} - b\beta',\, a, b \in \mathbb{Z} \right\} \\
&= \left\{ \left\lceil -\frac{1}{2} - b\beta' \right\rceil + b\beta \;\middle|\; b \in \mathbb{Z} \right\}
\end{aligned}$$

Thus we can express the sequence of points of the quasicrystal as:

$$y_n^{\left[-\frac{1}{2}, \frac{1}{2}\right)} = \left\lceil -\frac{1}{2} - n\beta' \right\rceil + n\beta$$

And for the set of distances between two consecutive points we have:

$$\begin{aligned}
\left\{ y_{n+1}^{\left[-\frac{1}{2}, \frac{1}{2}\right)} - y_n^{\left[-\frac{1}{2}, \frac{1}{2}\right)} \;\middle|\; n \in \mathbb{N} \right\} &= \left\{ \left\lceil -\frac{1}{2} - (n+1)\beta' \right\rceil + (n+1)\beta - \left\lceil -\frac{1}{2} - n\beta' \right\rceil - n\beta \;\middle|\; n \in \mathbb{Z} \right\} \\
&= \left\{ \left\lceil -\frac{1}{2} - (n+1)\beta' \right\rceil - \left\lceil -\frac{1}{2} - n\beta' \right\rceil + \beta \;\middle|\; n \in \mathbb{Z} \right\} \\
&= \left\{ \left\lceil -\frac{1}{2} - n\beta' - \beta' \right\rceil - \left\lceil -\frac{1}{2} - n\beta' \right\rceil + \beta \;\middle|\; n \in \mathbb{Z} \right\}
\end{aligned}$$

Because β is Pisot we have $|\beta'| < 1$. Therefore the difference between the ceilings is either 0 or ± 1 (the sign depends on the sign of β') and the set of distances between two consecutive points

thus collapses to simple $\{\beta, \beta \pm 1\}$. We want to be clear that here ± 1 means either $+1$ or -1 depending on the sign of β', the set of distances between two consecutive points will have two elements.

With a little thought and with the use of the scaling property of a qusicrystal we can expand this to any window of size β^k where $k \in \mathbb{Z}$.

$$\Sigma\left(\beta\left[-\frac{1}{2}, \frac{1}{2}\right)\right) = \beta'\Sigma\left(\left[-\frac{1}{2}, \frac{1}{2}\right)\right)$$

Thus for window $\left[-\frac{\beta^k}{2}, \frac{\beta^k}{2}\right)$ we have the set of distances between two consecutive points:

$$\left\{ y_{n+1}^{\left[-\frac{\beta^k}{2}, \frac{\beta^k}{2}\right)} - y_n^{\left[-\frac{\beta^k}{2}, \frac{\beta^k}{2}\right)} \;\middle|\; n \in \mathbb{N} \right\} = \left\{ \left|(\beta')^k \beta\right|, \left|(\beta')^k(\beta \pm 1)\right| \right\}$$

Now we utilize the fact, that β is a quadratic integer – i.e. root of polynomial $x^2 + bx + c$ for $b, c \in \mathbb{Z}$. Thus we can use Vietas's formulas and also $\beta = -b - \frac{c}{\beta}$.

Applying Vieta's formula ($\beta' = \frac{c}{\beta}$) we have:

$$\left\{ y_{n+1}^{\left[-\frac{\beta^k}{2}, \frac{\beta^k}{2}\right)} - y_n^{\left[-\frac{\beta^k}{2}, \frac{\beta^k}{2}\right)} \;\middle|\; n \in \mathbb{N} \right\} = \left\{ \left|\frac{c^k}{\beta^{k-1}}\right|, \left|\frac{c^k}{\beta^{k-1}} \pm \frac{c^k}{\beta^k}\right| \right\}$$

And applying $\frac{c}{\beta} = -\beta - b$ we get:

$$\begin{aligned}\left\{ y_{n+1}^{\left[-\frac{\beta^k}{2}, \frac{\beta^k}{2}\right)} - y_n^{\left[-\frac{\beta^k}{2}, \frac{\beta^k}{2}\right)} \;\middle|\; n \in \mathbb{N} \right\} &= \left\{ \left|(-1)^k \beta(\beta + b)^k\right|, \left|(-1)^k \beta(\beta + b)^k \pm (-1)^k(\beta + b)^k\right| \right\} \\ &= \left\{ \left|\beta(\beta + b)^k\right|, \left|(\beta \pm 1)(\beta + b)^k\right| \right\}\end{aligned}$$

In the scope of our interest we now know the set of distances between two consecutive points for window of size β: $\left\{\left|\beta^2 + b\beta\right|, |(\beta \pm 1)(\beta + b)|\right\}$ and just outside of our scope for window of size 1: $\{\beta, \beta \pm 1\}$. Now we need to expand this knowledge to the entire interval $(1, \beta]$.

It is possible to do this expansion for a general quadratic Pisot-cyclotomic β, as for example in [5]. We analyzed each β individually, however there are several facts that apply generally and are important for further progress:

- there are two or three different distances between two consecutive points of a quasicrystal, often denoted from smallest to largest as S, M and L
- the distances vary with different window length
- the star map images of points of a quasicrystal that precede certain distance form an interval

The last statement is of particular importance to us. In essence it means that there are one or two dividing points in the window of a quasicrystal that divide it into sections whose star map preimages precede the same distance in the quasicrystal. By extension it is also possible to divide the window by the distance that precede the preimage in the quasicrystal. We will explore this concept in greater detail later.

Based on these findings it is already possible to generate a finite section of a one dimensional quasicrystal.

- 0 is a fixed point of Galois isomorphism. 0 is also in every window centered around the origin (i.e. 0). Therefore 0 is present in every one dimensional quasicrystal with a window centered around it.
- We can acquire the next and previous points by identifying a section of a window the star map image of the point is present in followed by adding or subtracting appropriate distance.

For summary we outline the algorithm for acquiring arbitrary finite section of a one dimensional quasicrystal a bit more formally.

Input: window $[-\frac{\ell}{2}, \frac{\ell}{2})$; finite interval $[x_1, x_2]$

1. iterate through the points of the quasicrystal from 0 until you enter $[x_1, x_2]$
2. continue iterating while saving points in a list `quasicrystal` until you exit $[x_1, x_2]$

Output: the list `quasicrystal`

Thus we have accomplished the first step of our analysis. In the next section we will follow with the second step: estimating the covering radius of quasicrystal.

3.1.2 Estimate the covering radius R_C of the quasicrystal

The estimation is rather straight forward for the one dimensional case, it will be more complicated for the two dimensional case and we do it here for the sake of consistency.

Our definition of covering radius 1.3 simplified for one dimensional $D \subset \mathbb{R}$ would be:

$$R_C = \inf \{ r_2 > 0 \,|\forall x \in \mathbb{R} :\ B(x, r_2) \cap D \neq \emptyset \}$$

So we are looking for the upper bound on the largest possible distance to the nearest point of the quasicrystal from anywhere in $\mathbb{R}$.

As we have already found out in the previous section, there is a maximum distance between two consecutive points of the quasicrystal. Therefore the estimate we are looking for must be the half of the largest distance between two consecutive points.

$$\hat{R}_C = \frac{1}{2} \max_{n \in \mathbb{Z}} \{ y^{\Omega}_{n+1} - y^{\Omega}_{n} \}$$

In the next section we will use this estimate to generate a superset of all finite sections spanning $B(2\hat{R}_C)$.

3.1.3 Generate superset of all finite sections spanning $B(2\hat{R}_C)$

We want to briefly get back to our over all goal and explain the motivation behind this step in greater detail.

Our goal is to acquire the list of Voronoi tiles in one dimensional quasicrystal. It is possibly quite unusual to construct a Voronoi diagram on a one dimensional set. Once again we do it for consistency, however it also makes the presentation of results easier.

By Theorem 1.11 the domain of a Voronoi tile is limited by $B(x, 2\hat{R}_C)$ where x is the center of the tile. By constructing a Voronoi tile in every finite section spanning $B(2\hat{R}_C)$, we construct a Voronoi tile for every possible domain and by extension we have constructed every possible Voronoi tile. That is the motivation for this step.

Now let us continue with the exploration of one dimensional quasicrystal from Section 3.1.1. We are going to create an algorithm that will for given $n \in \mathbb{N}$ and window Ω return a list of finite sequences of $n+1$ points each, that entail all possible centered $n+1$ points long sequences of consecutive points of the quasicrystal (each sequence is centered around its middle point $y^{\Omega}_{i+\lfloor \frac{n}{2} \rfloor}$):

$$\left\{(y^{\Omega}_i - y^{\Omega}_{i+\lfloor \frac{n}{2} \rfloor}, y^{\Omega}_{i+1} - y^{\Omega}_{i+\lfloor \frac{n}{2} \rfloor}, \ldots, y^{\Omega}_{i+n+1} - y^{\Omega}_{i+\lfloor \frac{n}{2} \rfloor}) \,|\, i \in \mathbb{Z}\right\}$$

For that we introduce the notion of the stepping function of a quasicrystal.

Definition 3.2. Let $\Omega = [-\frac{\ell}{2}, \frac{\ell}{2})$ for $\ell \in \mathbb{Q}(\beta)$. The **stepping function** of the quasicrystal $\Sigma(\Omega)$ is the function $f^{\Omega} : \Omega \to \Omega$:

$$f^{\Omega}(y^{\Omega^*}_n) = {y^{\Omega}_{n+1}}^*$$

⌟

Remark. Note that the stepping function works with the star map images, not with the points of the quasicrystal.

The stepping function is a piecewise linear function. Each one of the two or three linear segments corresponds to one distance between the consecutive points of the quasicrystal. This aspect is what we are going to use for our algorithm. If we iterate the stepping function (i.e. $f^{\Omega} \circ f^{\Omega}$ or $(f^{\Omega})^2$) we of course get again a piecewise linear function, this time with more discontinuities. The linear segments now correspond to pairs of the distances between two consecutive points of the quasicrystal. Not only that, there is a linear segment for each possible pair of the distances. There is an illustration of the concept in Figure 3.2.

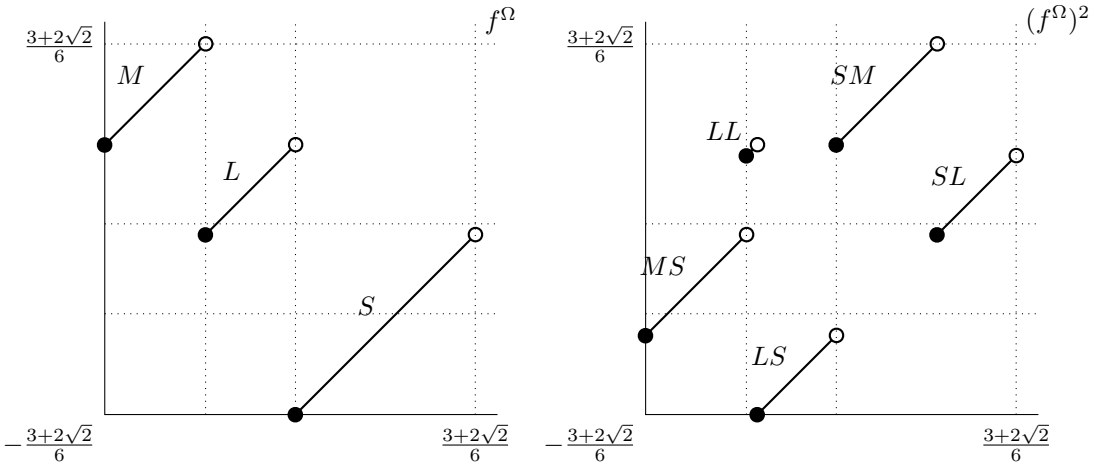

Figure 3.2: Example of the stepping function for $\beta_8 = 1+\sqrt{2}$ and window $\Omega = \left[-\frac{3+2\sqrt{2}}{6}, \frac{3+2\sqrt{2}}{6}\right)$. On the left there is just the stepping function and on the right there is its second iteration. Letters S, M, L mark different lengths of distances.

Now the algorithm should be quite obvious. We are going to iterate the stepping function n times and from each finite sequence of the distances construct a finite section of $n+1$ points of the quasicrystal.

Again we summarize with a more detailed description of the algorithm.

Input: window $[-\frac{\ell}{2}, \frac{\ell}{2})$; number $n \in \mathbb{N}$

1. save the three linear segments of $f^{\Omega}(\Omega)$ as intervals in a list `segments`, mark each with the corresponding distance
2. repeat $n-1$ times: for each interval $I \in$ `segments` save the linear segments of $f^{\Omega}(I)$, append the marks accordingly

Output: list of marks of intervals from `segments`

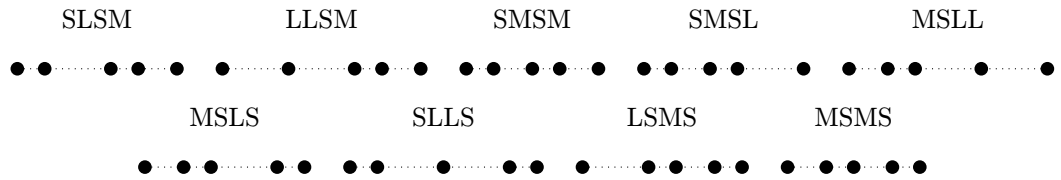

Figure 3.3: Example of the list of sequences of distances for $\beta_8 = 1+\sqrt{2}$, $n=4$ and window $\Omega = \left[-\frac{3+2\sqrt{2}}{6}, \frac{3+2\sqrt{2}}{6}\right)$. Letters S, M, L mark different lengths of distances. $S=1$, $M=\beta_8-1$ and $L=\beta_8$. Below each sequence of distances is the created finite section of the quasicrystal.

Once we acquire the list of sequences of distances, we easily convert them to sequences of points of the quasicrystal. There is an example of the algorithm output and this conversion in Figure 3.3. Now it remains to establish n such that the sequences of points of the quasicrystal have sufficient length.

We want the finite sections to span $B(2\hat{R}_C)$, in other words we want the finite sections to be at least $4\hat{R}_C$ long. The obvious solution is to run the algorithm for $n=1$ measure the shortest sequence and if it is shorter than $4\hat{R}_C$, increase n by 1, run the algorithm again and repeat until we acquire not only the n but also the list of the finite sequences of sufficient length.

It is also beneficial to choose an even n, that will result in odd number of points in the finite sections and that will ease the next step. Although it might result in the finite sections being longer than necessary.

Thus we have accomplished the third step of analysis and we can move on the next step.

3.1.4 Filter the superset to the final list of Voronoi tiles

First we have to turn the list of finite sections from the previous step into a list of Voronoi tiles. Rather simply we just pick a point in each finite section as a center of the Voronoi tile. Here we see the benefit of having an odd number of points, since we can just pick the middle point. Constructing a Voronoi cell is then straight forward.

As we can see in the example in Figure 3.4, several tiles appear multiple times, that is intrinsic to our method. Now we can simply select unique Voronoi tiles and present the tiles just with their domains (Figure 3.5).

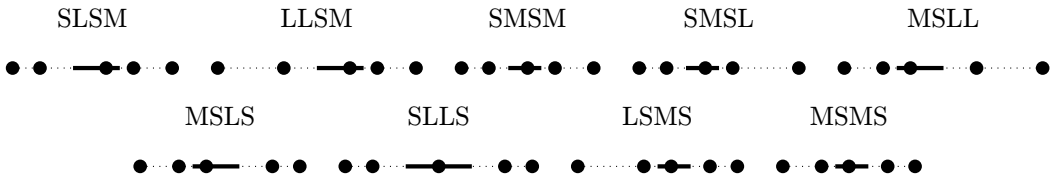

Figure 3.4: Example of the Voronois tiles on the list of finite sections of the quasicrystal for $\beta_8 = 1 + \sqrt{2}$, $n = 4$ and window $\Omega = \left[-\frac{3+2\sqrt{2}}{6}, \frac{3+2\sqrt{2}}{6}\right)$. Voronoi tiles are represented by the thick line.

Figure 3.5: Example of unique Voronois tiles (from Figure 3.4) with their domains from the quasicrystal for $\beta_8 = 1 + \sqrt{2}$, $n = 4$ and window $\Omega = \left[-\frac{3+2\sqrt{2}}{6}, \frac{3+2\sqrt{2}}{6}\right)$. Voronoi tiles are represented by the thick line.

It may seem that the analysis ends here, however even though it did not happen in our example it might happen for two dimensional window that the acquired list of Voronoi tiles contains tiles that do not actually appear in the quasicrystal. We want to present our method for dealing with such eventuality here, since it is much easier to understand with one dimensional Voronoi tiles but is directly applicable to two dimensional Voronoi tiles as well.

For demonstration, let us add to our example list two more Voronoi tiles that we will eventually identify and remove (Figure 3.6). We will regard these added Voronoi tiles as artificial.

Figure 3.6: Example of the Voronois tiles with their domains from the quasicrystal for $\beta_8 = 1 + \sqrt{2}$, $n = 4$ and window $\Omega = \left[-\frac{3+2\sqrt{2}}{6}, \frac{3+2\sqrt{2}}{6}\right)$ with **two extra** Voronoi tiles that do not appear in the quasicrystal.

Now we will explore the relationship between a Voronoi tile $V(x)$ and the window Ω of the quasicrystal. For the Voronoi tile to exist in the quasicrystal the star map images of its center x and domain $D(x)$ must fit inside the window Ω. Let us denote the points of the domain as $\{d_1, \ldots, d_k\} = D(x)$.

$$x^* \in \Omega \quad \wedge \quad d_i^* \in \Omega \quad \forall i \in \hat{k}$$

For centered domain $q_i = d_i - x$, $\forall i \in \hat{k}$ we get:

$$x^* \in \Omega \quad \wedge \quad x^* \in \Omega - q_i^* \quad \forall i \in \hat{k}$$

$$x^* \in \Omega|_{V(x)} \stackrel{\text{def}}{=} \bigcap_{i \in \hat{k}} (\Omega - q_i^*) \cap \Omega$$

This is very important, we have now turned the question whether a Voronoi tile could appear in the quasicrystal into the question whether an intersection of several translated windows $\Omega|_{V(x)}$ is empty.

Now we can for each of the Voronoi tiles on our list construct such intersection and find out whether it is empty. It just happens that the section of the smallest Voronoi tile is empty (Figure 3.7).

Figure 3.7: Example of the elimination of a Voronoi tile by window intersection. This tile would be eliminated.

Just for illustration we also show the intersection of one of the tiles that appears in the quasicrystal (Figure 3.8).

Figure 3.8: Example of the elimination of a Voronoi tile by window intersection. This tile would pass.

The second Voronoi tile we artificially added does however pass this filter. To get the final list of Voronoi tiles of the quasicrystal, we have to again look at the window.

The intersection we used to eliminate some of the tiles contains more information. A point of quasicrystal whose star map image fits in the intersection will be surrounded by the corresponding domain:

$$x \in \Sigma(\Omega) \quad \wedge \quad x^* \in \bigcap_{i \in \hat{k}} (\Omega - q_i^*) \cap \Omega \qquad \Rightarrow \qquad x + q_i \in \Sigma(\Omega) \quad \forall\, i \in \hat{k}$$

That however does not yet define the Voronoi tile that belongs to the point x. The intersections for various Voronoi tiles may overlap. A point of quasicrystal whose star map image fits in multiple intersections will be surrounded by multiple domains and thus the resulting Voronoi tile will be the smallest one of the acceptable ones.

We illustrate this process with two figures. Figure 3.9 shows a list of Voronoi tiles with corresponding window intersections. Note that the intersections do overlap.

Figure 3.10 shows that the smallest tile will indeed be the one that appears in the quasicrystal.

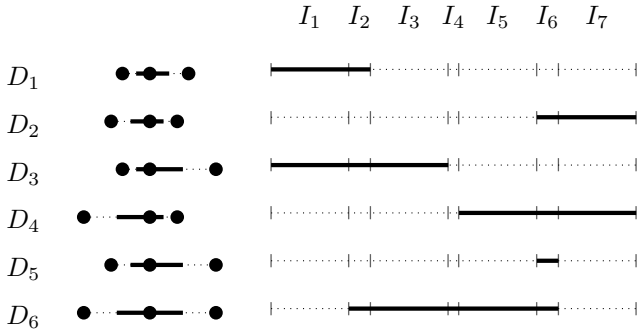

Figure 3.9: List of Voronoi tiles with corresponding window intersections. The tiles are sorted from top to bottom by increasing size.

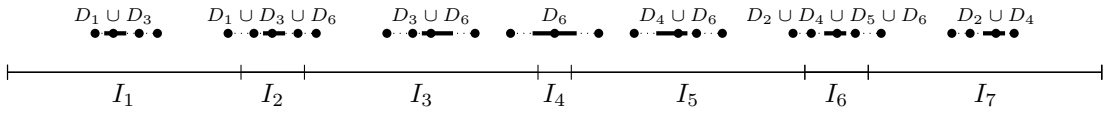

Figure 3.10: A window of a quasicrystal divided by overlapping intersections from Figure 3.9. Voronoi tile above each section shows which Voronoi tile would appear in the quasicrystal.

We can also see that the second artificially added Voronoi tile with the domain D_5 does not pass this filter since it is bigger than other Voronoi tiles (with domains D_2 and D_4) whose intersections are supersets of the intersection of the artificial Voronoi tile. It could also happen that the intersection would be covered by multiple intersections of smaller Voronoi tiles. In this context covered means that for each point in the intersection of the artificial Voronoi tile there is an intersections of smaller Voronoi tile that also contains said point.

That brings us to the idea that we could divide the window of a quasicrystal into sections corresponding to different Voronoi tiles. Each intersection $\Omega|_{V(x)}$ just needs to be adjusted by intersections of smaller Voronoi tiles U:

$$\Phi(V) \stackrel{\text{def}}{=} \Omega|_V \setminus \bigcup_{|U|<|V|} \Omega|_U$$

This division is illustrated by Figure 3.11. And of course a Voronoi tile V whose section $\Phi(V)$ is empty does not appear in the quasicrystal.

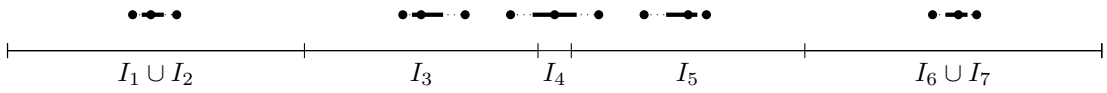

Figure 3.11: A window of a quasicrystal divided into sections corresponding to different Voronoi tiles.

All together this last step of the analysis consists of three filters:

1. Eliminate duplicate Voronoi tiles.
2. Eliminate Voronoi tiles whose intersection $\Omega|_V = \bigcap_{i \in \hat{k}} (\Omega - q_i^*) \cap \Omega$ is empty.
3. Eliminate Voronoi tiles whose section $\Phi(V) = \Omega|_V \setminus \bigcup_{|U|<|V|} \Omega|_U$ is empty.

3.1.5 Establish the period of each Voronoi tile

Now that we are able to acquire a list of Voronoi tiles for a quasicrystal with one dimensional window, it is time to explore changes in the list with changing window size.

As per usual there are many ways to solve this. The method presented here is again as general as we could find. After we describe this general method on a simple one dimensional case, we will also show a much easier method that is however not applicable to two dimensional quasicrystals.

Now assume we have a window Ω and the list of Voronoi tiles of the quasicrystal $\Sigma(\Omega)$: $\Psi(\Omega) = \{V_1, \ldots, V_k\}$ for $k \in \mathbb{N}$.

Our method relies on our ability to calculate area of the section of the window of the quasicrystal that corresponds to a certain Voronoi tile $V \in \Psi(\Omega)$:

$$\Phi(V) = \Omega|_V \setminus \bigcup_{\substack{U \in \Psi(\Omega) \\ |U|<|V|}} \Omega|_U$$

Due to constraints of specific windows, it might not be possible or practical to directly calculate area of union of intersections. However, if we are able to calculate the area of $\Omega|_V$ (i.e. the area of the intersection of several translated windows Ω), we can use the inclusion–exclusion principle to calculate area of the union. Let us denote the list of Voronoi tiles smaller than $V \in \Psi(\Omega)$ as $Q_V = \{U \in \Psi(\Omega) : |U| < |V|\}$. We will use $A(\cdot)$ to mark when we calculate the area of a set.

$$A\left(\bigcup_{U \in Q_V} \Omega|_U\right) = \sum_{U \in Q_V} A\big(\Omega|_U\big) - \sum_{\substack{U,W \in Q_V \\ |U|<|W|}} A\big(\Omega|_U \cap \Omega|_W\big) + \sum_{\substack{U,W,R \in Q_V \\ |U|<|W|<|R|}} A\big(\Omega|_U \cap \Omega|_W \cap \Omega|_R\big) - \cdots + (-1)^{|Q_V|-1} A\left(\bigcap_{U \in Q_V} \Omega|_U\right)$$

It might look a bit complicated but it is an algorithmic way for calculating an area of the union through addition and subtraction of areas of intersections, which we found as generally easier than directly calculating the area of the union. Thus we are now capable of calculating the area of $\Phi(V)$ for any $V \in \Psi(\Omega)$.

We can of course scale a window Ω by $\omega \in \mathbb{R}$: $\omega\Omega$. If $|\Omega| = 1$ we can regard ω as the size of window $\omega\Omega$. Thus further in this section we will assume $|\Omega| = 1$.

Now we shall use the capability to calculate area of a union to find the infimum $\omega_1 \in \mathbb{R}$ of window Ω sizes such that the Voronoi tile V appears in the corresponding quasicrystal and the supremum $\omega_2 \in \mathbb{R}$ of window Ω sizes such that the Voronoi tile V appears in the corresponding quasicrystal:

$$\omega_1 = \inf\{\omega \in \mathbb{R} \,|\, V \in \Psi(\omega\Omega)\} \qquad \omega_2 = \sup\{\omega \in \mathbb{R} \,|\, V \in \Psi(\omega\Omega)\}$$

This of course means that the Voronoi tile V might not appear in quasicrystals $\Sigma(\omega_1\Omega)$ and $\Sigma(\omega_2\Omega)$.

The intersection $\Omega|_V$ is created by translating several windows Ω by the star map images of V's domain. Here the important aspect is that the domain of V as well as the star map images are independent of Ω. So we can easily explore how does the area of $(\omega\Omega)|_V$ change with $\omega \in \mathbb{R}$:

$$(\omega\Omega)|_V = \bigcap_{i \in \hat{k}} (\omega\Omega - q_i^*) \cap \omega\Omega$$

where $\{q_1, \ldots, q_k\}$ is the domain of V. The important aspect here is that the area of the intersection changes with the same rate as the area of $\omega\Omega$.

Thus we can reverse engineer the formula for calculating $A((\omega\Omega)|_V)$ from ω and find ω_1 as the largest ω for which the area $A((\omega\Omega)|_V)$ is zero.

Similarly thanks to the inclusion–exclusion principle we can reverse engineer the formula for calculating $A(\Phi(V))$ for variable window size and find ω_2 as the smallest $\omega > \omega_1$ for which

the area $A(\Phi(V))$ is zero. In this case however a greater care is necessary, since $A(\Phi(V))$ for increasing window size first increases and only after a certain window size it starts to decrease and it is the rate of this decrease that we are interested in.

Example in one dimension

To show our method we will calculate ω_1 and ω_2 for this Voronoi tile V from our example:

Figure 3.12: Voronoi tile V.

We will use $\beta_8 = 1 + \sqrt{2}$ to denote the Pisot-cyclotomic number that the quasicrystal is associated to. Let $\Omega = [\frac{1}{2}, \frac{1}{2})$ be interval of length 1 and $\omega \in \mathbb{R}$. Obviously an interval's size changes linearly with its length. Thus we will assume following formula for the area of interval intersection:

$$A = a(\omega + d) \quad \text{for} \quad a, d \in \mathbb{R}$$

If we know two pairs of ω and area of corresponding interval intersection, we can calculate a and d:

$$(x_1, A_1) \qquad (x_2, A_2)$$
$$a = \frac{A_1 - A_2}{x_1 - x_2} \qquad d = \frac{A_1}{a} - x_1$$

Now to get ω_1 we calculate the area $A((\omega\Omega)|_V)$ for two different values of ω and use the formulas above:

$$x_1 = 1 \qquad A_1 = 5 - 2\beta_8$$
$$x_2 = \beta_8 - 1 \qquad A_2 = 3 - \beta_8$$

$$a = \frac{5 - 2\beta_8 - 3 + \beta_8}{1 - \beta_8 + 1\beta_8 + 3} = 1$$
$$d = 5 - 2\beta_8 - 1 = 4 - 2\beta_8$$

We are looking for the area $A((\omega\Omega)|_V)$ to be zero:

$$\omega_1 + d = 0 \quad \Rightarrow \quad \omega_1 = 2\beta_8 - 4$$

To get ω_2 we calculate the area $A(\Phi(V))$ for two different values of ω and again use the formulas above:

$$x_1 = \frac{2\beta_8}{3} \qquad A_1 = \frac{6 - 2\beta_8}{3}$$
$$x_2 = \frac{\beta_8 + 3}{3} \qquad A_2 = \frac{3 - \beta_8}{3}$$

$$a = \frac{6 - 2\beta_8 + \beta_8 - 3}{2\beta_8 - \beta_8 - 3} = -1$$

$$d = \frac{2\beta_8 - 6}{3} - \frac{2\beta_8}{3} = -2$$

Again we are looking for the area $A(\Phi(V))$ to be zero:

$$\omega_2 + d = 0 \quad \Rightarrow \quad \omega_2 = 2$$

Thus according to our method the Voronoi tile V first appears in quasicrystals with windows greater than $\omega_1\Omega = [\beta_8 - 2, \beta_8 - 2)$ and disappears just before window $\omega_2\Omega = [1, 1)$. Which is also in accordance with the second method we will show, that is however only applicable to one dimensional quasicrystals.

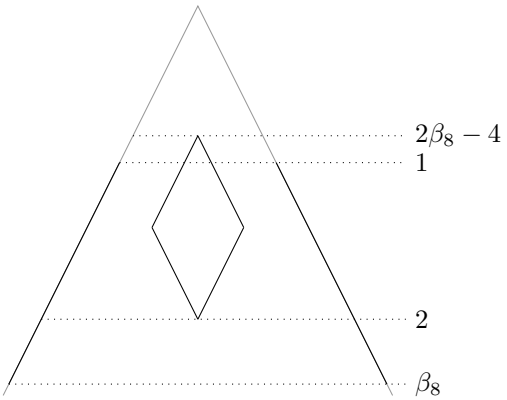

Figure 3.13: The section $\Phi(V)$ for Voronoi tile in Figure 3.12 for window sizes in $[2\beta_8 - 4, \beta_8]$. Horizontal slices represent the window of each size and the rhombus show the increasing and decreasing size of the section $\Phi(V)$. Note that $2\beta_8 - 4$ is outside the interval $(1, \beta_8]$.

Easier method for one dimensional quasicrystals

For the case of one dimensional quasicrystal we can calculate ω_1 and ω_2 for each Voronoi tile at the same time thanks to the stepping function. We have already used the stepping function to generate a superset of all finite sections for a given window. There we have discovered that the stepping function's and its iteration's discontinuities divide the window by corresponding finite sections of distances between two consecutive points of the quasicrystal. Now we want to explore how these discontinuities and the finite sections of distances between two consecutive points evolve with changing window size.

If we plot the points of discontinuity as a function of the size of the window (Figure 3.14), we observe that there are window sizes having divisions very different to divisions of windows with similar size. These are marked with dotted line in Figure 3.14.

Now we describe the concept a bit more formally. Let us denote $d_{n,1}(\omega) \leq \cdots \leq d_{n,k}(\omega)$ the points discontinuity of the nth iteration of the stepping function $(f^{\omega\Omega})^n$ as functions of the window size $\omega \in (1, \beta]$, where $|\Omega| = 1$. As we see in Figure 3.15, these functions also have discontinuities and are also piece-wise linear. (In Figure 3.15 the linear segments are divided by $\beta_8 - 1$ and for the second iteration also 2.)

The point of this confusing exercise is the following:

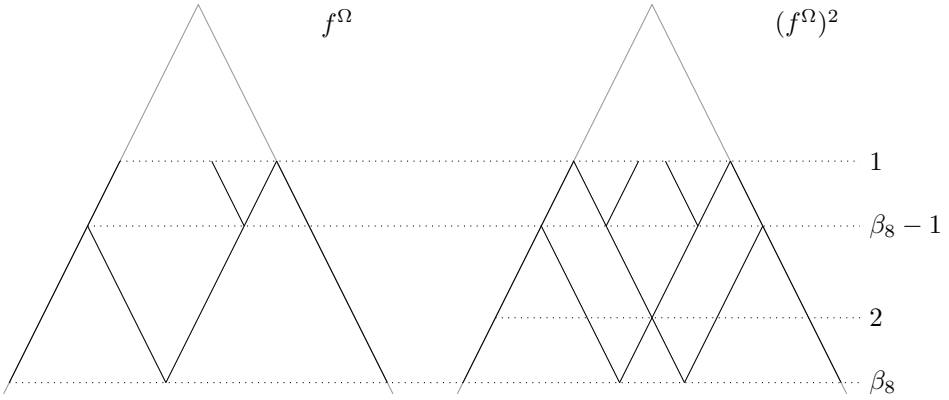

Figure 3.14: Discontinuities of the stepping function f^Ω and its second iteration $(f^\Omega)^2$ as a function of the size of the window Ω for window size in $(1, \beta_8]$ where $\beta_8 = 1 + \sqrt{2}$.

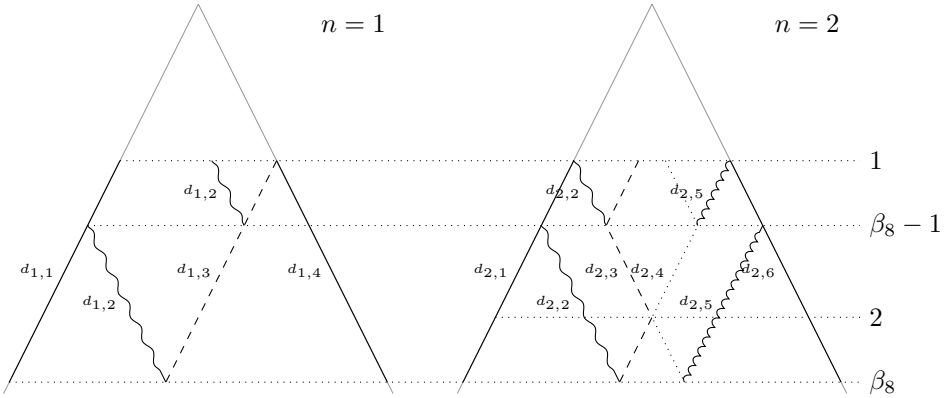

Figure 3.15: Plots of functions $d_{n,1}(\omega), \ldots, d_{n,k}(\omega)$ for $n = 1$ and $n = 2$.

- inside their segments of linearity the functions $d_{n,1}(\omega), \ldots, d_{n,k}(\omega)$ divide the window in the same number of sections corresponding to the same lists of sequences of distances

- the windows of sizes where at least one of the functions $d_{n,1}(\omega), \ldots, d_{n,k}(\omega)$ ends its segment of linearity are divided in smaller number of sections corresponding to unique list of sequences of distances

As we have observed in our examples in previous section, each Voronoi tile corresponds uniquely to only a pair of distances (i.e. a sequence of distances of length two). Thus it is sufficient to only do one iteration of the stepping function $(f^\Omega)^2$ and the ends of linear segments of $d_{2,1}(\omega), \ldots, d_{2,k}(\omega)$ are a union of the ω_1s and ω_2s for each Voronoi tile that appears in a quasicrystal with sindow size in $(1, \beta]$.

That concludes our analysis of one dimensional quasicrystals. Next we will continue with the analysis of quasicrystals with two dimensional windows. Results of our analysis applied to one dimensional quasicrystals can be seen in Chapter 4.

3.2 Two dimensional quasicrystal

Now that we have analyzed quasicrystals with one dimensional windows and perhaps more importantly we have seen our method of analysis in action it is time to analyze quasicrystals with two dimensional windows.

First we recapitulate various components of our quasicrystal model (in its entirety in Definition 2.3).

Let $n \in \mathbb{N}\setminus\{2,3,4,6\}$. Let β be a quadratic Pisot-cyclotomic number of order n, associated to $\rho = 2\cos(2\pi/n)$. Further, let $* : \mathbb{R}^2 \to \mathbb{R}^2$ be defined as $(x,y)^* = (\Re\big((x+iy)^{*^{\mathbb{C}}}\big), \Im\big((x+iy)^{*^{\mathbb{C}}}\big))$ where $*^{\mathbb{C}}$ is an appropriate Galois isomorphism of $\zeta = e^{2\pi\mathrm{i}/n}$. Let $v_1, v_2 \in \mathbb{R}^2$:

$$v_1 = (1,0) \quad \text{and} \quad v_2 = (\Re(\zeta), \Im(\zeta))$$

and let $M = \mathbb{Z}[\beta]\, v_1 + \mathbb{Z}[\beta]\, v_2$ and $N = \mathbb{Z}[\beta]\, v_1^* + \mathbb{Z}[\beta]\, v_2^*$. Lastly let $\Omega \subset N$ be bounded with nonempty interior.

The model of two dimensional quasicrystal linked to irrationality β and window Ω is the set:

$$\Sigma(\Omega) = \{x \in M \mid x^* \in \Omega\}$$

We will use the notation from above to denote the same objects in the rest of this chapter.

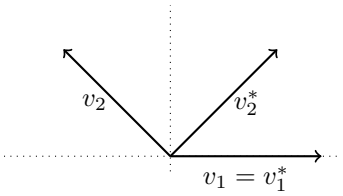

Figure 3.16: Example of the vectors v_1, v_2, v_1^* and v_2^* for Pisot-cyclotomic $\beta_8 = 1+\sqrt{2}$.

As we hinted before we will analyze two dimensional quasicrystals just for several specific windows.

Definition 3.3. Let $\Omega \subset \mathbb{R}^2$:
$\Omega = Iv_1^* + Iv_2^*$ where I is a left-closed right-open interval is a **rhombic window**.
Ω equal to closed convex hull of $\big\{\big(\cos(2k\pi/n), \sin(2k\pi/n)\big) \big| k = 0, \ldots, n-1\big\}$ for $n \in \mathbb{N}$ is a **n-gonal window**.
$\Omega = \{x \in \mathbb{R}^2 \mid \|x\| \leq R\}$ where $R > 0$ is a **circular window**. ⌟

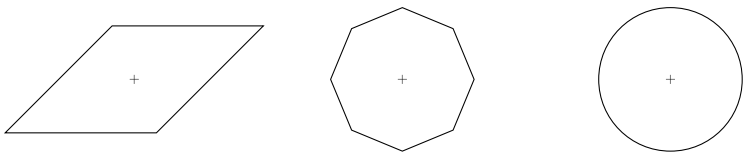

Figure 3.17: Example of three window shapes: rhombic, octagonal and circular windows for Pisot-cyclotomic $\beta_8 = 1+\sqrt{2}$.

Now we explain why we did analyze the one dimensional quasicrystal first. Since we used cut-and-project scheme for our model of a quasicrystal it is possible to decompose a quasicrystal

with rhombic window into two quasicrystals with one dimensional windows.

$$\Sigma(Iv_1^* + Iv_2^*) = \Sigma(I)v_1 + \Sigma(I)v_2$$

Here we see why a rhombic window has different closeness to the other windows we consider, it stems right from this decomposition and the left-closed right-open intervals.

Equipped with this very handy decomposition we are ready to start the analysis of two dimensional quasicrystal with the first step.

3.2.1 Arbitrary finite section

There are two concepts vitally important to this step. The decomposition we just saw and the inclusion property. First let us explain how to acquire arbitrary finite section of a quasicrystal with a rhombic window.

Input: rhombic window $Iv_1^* + Iv_2^*$; finite intervals $[x_1, x_2]$, $[y_1, y_2]$

1. acquire finite section of one dimensional quasicrystal with window I and interval $[x_1, x_2]$, save in `quasicrystal01`
2. acquire finite section of one dimensional quasicrystal with window I and interval $[y_1, y_2]$, save in `quasicrystal02`
3. compose list `quasicrystal` as points $z = x \cdot v_1 + y \cdot v_2$ for $x \in$ `quasicrystal01` and $y \in$ `quasicrystal02`

Output: the list `quasicrystal`

This algorithm however might not work as we expect. Since v_1 and v_2 are not perpendicular the returned finite section is not the intersection of the quasicrystal with a rectangle (i.e. $\Sigma(Iv_1^* + Iv_2^*) \cap [x_1, x_2] \times [y_1, y_2]$) but is also of the shape of a rhombus. This is simply solved by acquiring larger finite section and cropping it to fit the desired rectangle. There is an example of such finite section in Figure 3.18.

Now we use the inclusion property to generalize the algorithm for any window Ω. As a reminder the inclusion property is:

$$\Omega_1 \subset \Omega_2 \quad \Rightarrow \quad \Sigma(\Omega_1) \subset \Sigma(\Omega_2)$$

Thus it is enough to circumscribe a rhombus $(Iv_1^* + Iv_2^*)$ to whatever window we desire, use the algorithm to acquire a finite section of a quasicrystal with the rhombic window and then check for each point whether its star map image fits inside the desired window:

$$\Sigma(\Omega) = \{x \in \Sigma(Iv_1^* + Iv_2^*) \mid x^* \in \Omega\}$$

There is an example of this process in Figure 3.19.

To summarize, we are able to acquire a finite section of a quasicrystal with a rhombic window by composing two finite sections of a quasicrystal with one dimensional window. Through a finite section of a quasicrystal with a rhombic window we are able to acquire a finite section of a quasicrystal with any other window thanks to the inclusion property.

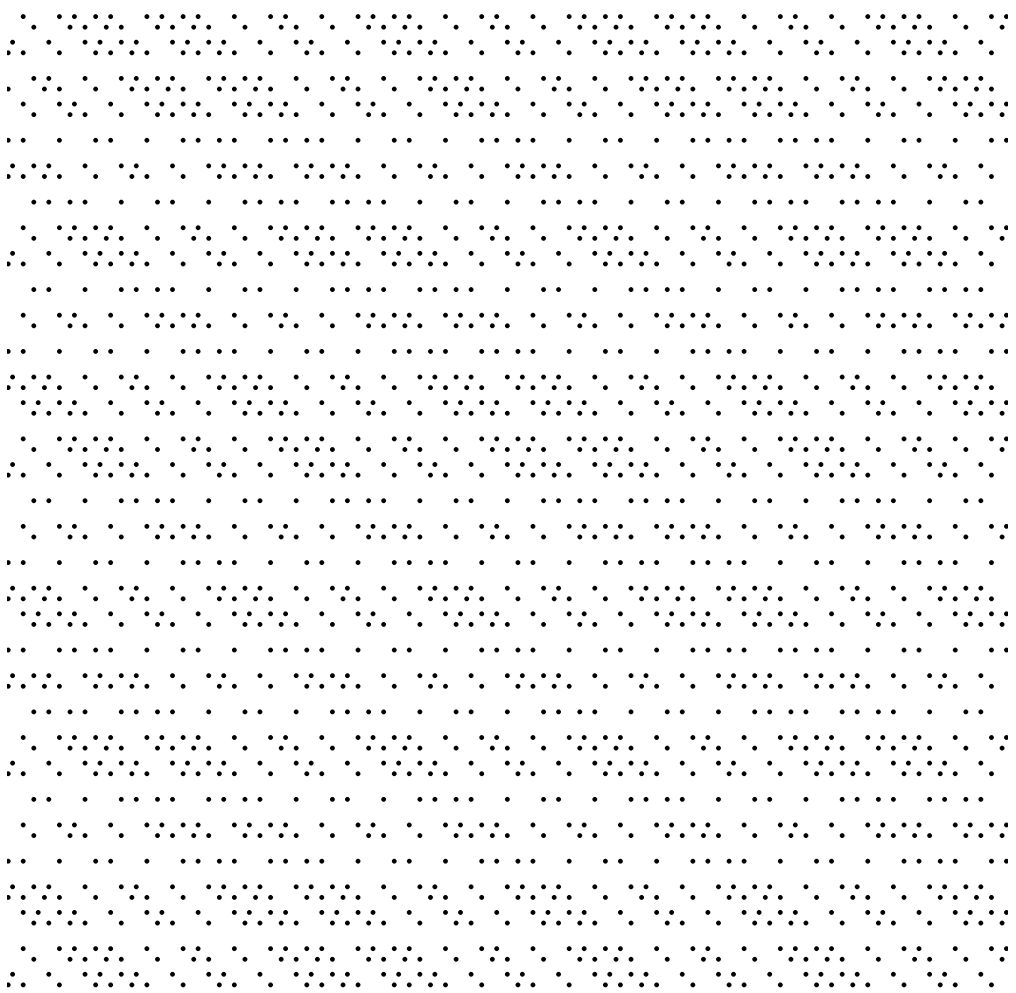

Figure 3.18: Example of a finite section of a two dimensional quasicrystal with a rhombic window for Pisot-cyclotomic $\beta_8 = 1 + \sqrt{2}$.

3.2.2 Estimate covering radius of the quasicrystal R_C

There is much to gain from a proper covering radius estimate since it can greatly reduce the number of cases considered in the next step. We have tried several different ways to acquire the estimate. The method we present here worked the best for us.

As a reminder here is the covering radius definition, simplified for two dimensions:
The **covering radius** of a set $D \subset \mathbb{R}^2$ is the number:

$$R_C = \inf \left\{ r_2 > 0 \;\middle|\; \forall\, z \in \mathbb{R}^2 :\; B(z, r_2) \cap D \neq \emptyset \right\}$$

By Theorem 1.12 we also have a way to calculate the covering radius from a Voronoi diagram:

$$R_C = \sup_{x \in D} \left\{ \sup_{y \in V(x)} \|y - x\| \right\}$$

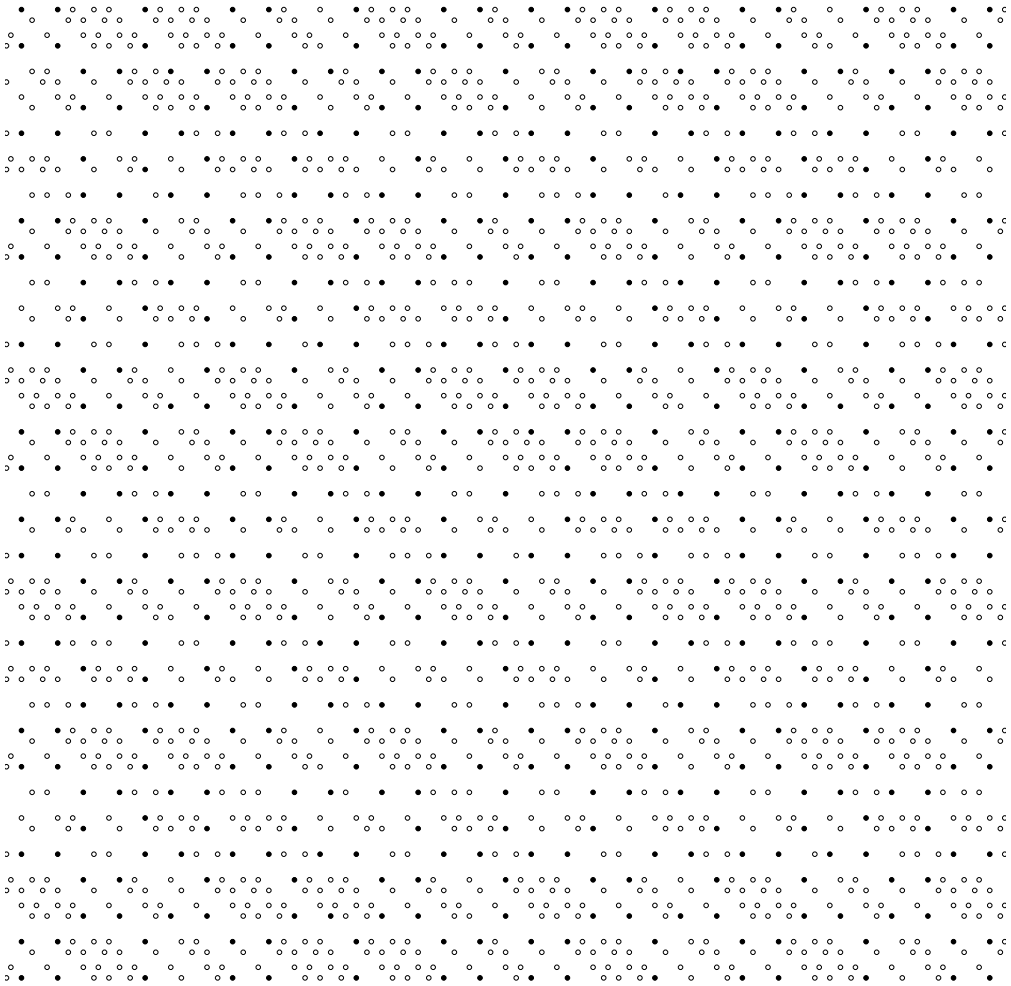

Figure 3.19: Example of a finite section of a two dimensional quasicrystal with an octagonal window for Pisot-cyclotomic $\beta_8 = 1 + \sqrt{2}$. The $\bullet$ points are the points of the quasicrystal with octagonal window and the $\circ$ and $\bullet$ points are points of the quasicrystal with a rhombic window circumscribed to the octagonal window. (Figure 3.18)

Here we run in a bit of a problem. The formula we suggested requires the list of Voronoi tiles that we do not know yet. In fact we want to use the covering radius estimate to acquire the list of Voronoi tiles. Luckily, there is a workaround. We do not actually need the complete list of Voronoi tiles to use the formula, just the one Voronoi tile that has the largest radius. There is a way to ensure we have the one tile without knowing the complete list of Voronoi tiles.

First we need a way to acquire even an incomplete list of Voronoi tiles. We construct a Voronoi diagram of a finite section of the quasicrystal (described in previous step). That will result in possibly incomplete list of Voronoi tiles, the completeness depends on the size of the finite section.

Now we need to make sure our possibly incomplete list of Voronoi tiles contains the one

Voronoi tile with the largest radius. There is a way to show that any Voronoi tile that might be missing has smaller radius than at least one Voronoi tile already on the list. We recall the analysis of quasicrystals with one dimensional windows. There we have divided a window into sections corresponding to various Voronoi tiles. We can create the division of the window even with an incomplete list of Voronoi tiles. If the union of the sections $\Omega|_V$ is the entire window Ω, our list of Voronoi tiles is sufficient for covering radius estimation. Now we look at this idea in greater detail.

Assume a list of Voronoi tiles $\{V_1, \ldots, V_m\}$, that may be incomplete. For each of the Voronoi tiles with domains $D_i = \{q_{i,1}, \ldots, q_{i,k_i}\}$ construct the following intersection:

$$\Omega|_{V_i} = \bigcap_{j \in \hat{k_i}} (\Omega - q^*_{i,j}) \cap \Omega$$

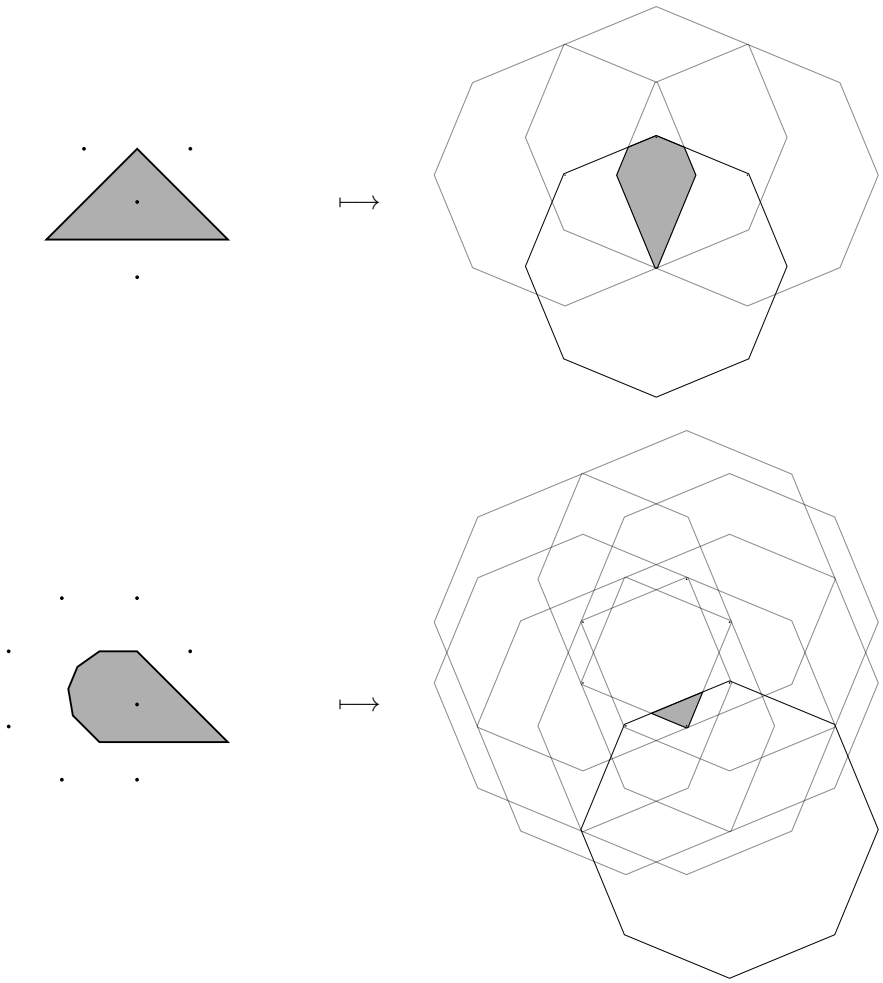

Figure 3.20: Example of window intersectios for two Voronoi tiles.

As we have discussed previously a point of the quasicrystal whose star map image fits in one of these intersections is surrounded by the corresponding domain. If several of these intersections

overlap, a point whose star map image fits in the intersection of the intersections is surrounded by several domains.

Once our list of Voronoi tiles $\{V_1, \ldots, V_m\}$ covers the window by its intersections:

$$\Omega = \bigcup_{i \in \hat{m}} \Omega|_{V_i}$$

any missing Voronoi tile's intersections would overlap the current ones and thus the missing Voronoi tile would have a smaller radius.

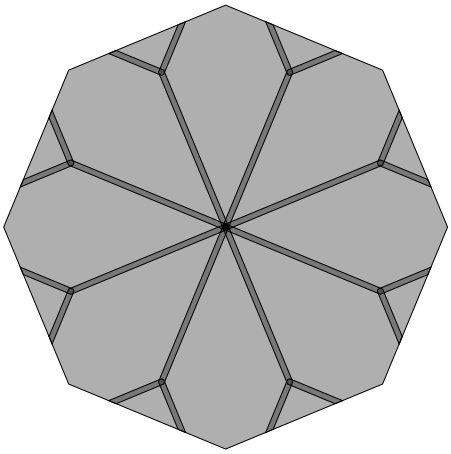

Figure 3.21: Example of a octagonal window covered by intersections of only sixteen Voronoi tiles including the two from Figure 3.20 (there are many more in the quasicrystal).

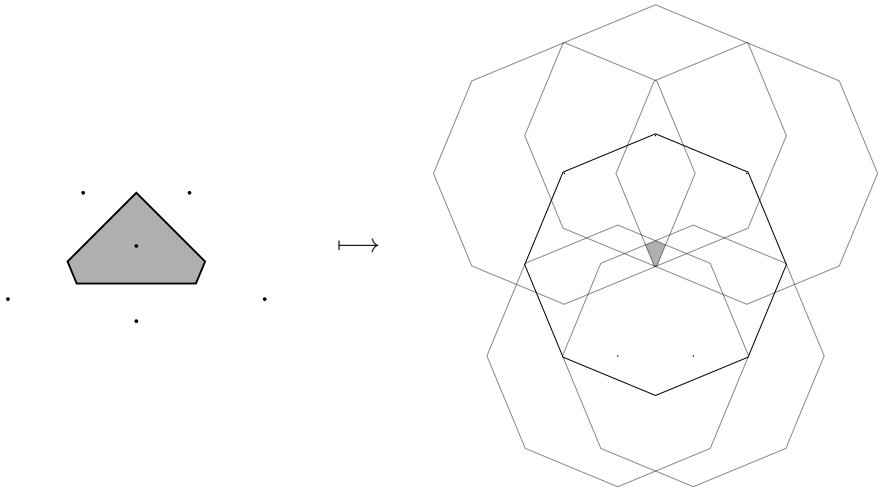

Figure 3.22: Example of a Voronoi tile whose intersection would overlap one of the intersections in Figure 3.21 and it indeed has smaller radius than the two considered Voronoi tiles in Figure 3.20.

To summarize, assume a list of Voronoi tiles $\{V_1, \ldots, V_m\}$, that may be incomplete, with domains $D_i = \{q_{i,1}, \ldots, q_{i,k_i}\}$. Then given another condition the estimate $\hat{R}_C$ of covering radius

R_C is obtained as:

$$\Omega = \bigcup_{i \in \hat{m}} \Omega|_{V_i} \qquad \Rightarrow \qquad \hat{R}_C \stackrel{\text{def}}{=} R_C = \max_{i \in \hat{m}} \left\{ \sup_{y \in V_i} \|y\| \right\}$$

The series of articles [6], [7] and [8] that our work is based upon, used an easier method for covering radius estimation that results in a worse estimate than the method we have just described. Since the quasicrystals we are analyzing have higher complexity, improving the covering radius estimate in this way was absolutely vital to completion of our analysis.

3.2.3 Generate superset of all finite sections spanning $B(2\hat{R}_C)$

This step is also solved by the rhombus decomposition and the inclusion property. Previously we have developed an algorithm to acquire all possible finite sections of a quasicrystal with one dimensional window spanning a given length. If we compose each pair of these into finite sections of a quasicrystal with rhombic window, we acquire a list of all possible finite sections spanning a rhombic area. Thus the length given to the algorithm to acquire all possible finite sections of a quasicrystal with one dimensional window must be the length of an edge of a rhombus circumscribed to $B(2\hat{R}_C)$.

Finding a formula to calculate the length of an edge of the rhombus a circumscribed to $B(2\hat{R}_C)$ from $\hat{R}_C$ is just a trigonometric exercise and we will not cover it here. The formula is:

$$a^2 = \frac{16\hat{R}_C^2}{\left(1 + \frac{\rho}{2}\right)\left(1 - \frac{\rho}{2}\right)}$$

where ρ is the $\rho = 2\cos(2\pi/n)$ to which β is associated.

Once we calculate a we can acquire all possible finite sections of a quasicrystal with one dimensional window spanning a and then for each pair compose a finite section of the quasicrystal with the rhombic window. Of course we can also crop these by $B(2\hat{R}_C)$.

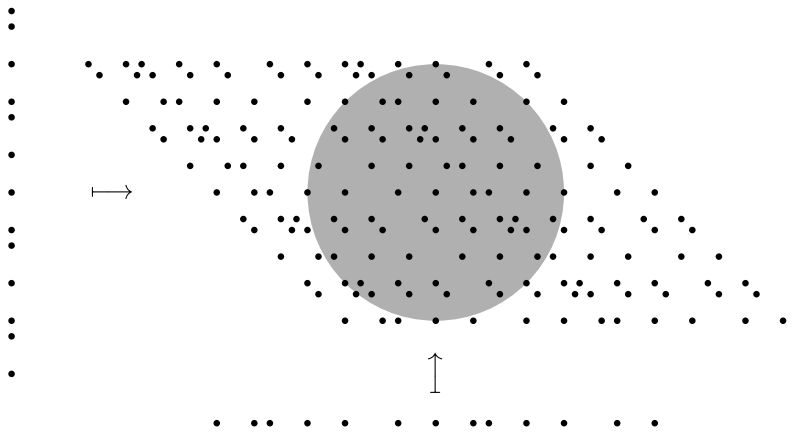

Figure 3.23: Example of the composition of a finite section of a quasicrystal with a rhombic window from two finite section of a quasicrystal with one dimensional window. The circle has radius $2\hat{R}_C$.

That completes the task of acquiring a list of all possible finite sections of a qusicrystal with a rhombic window, the easy part of this step. Now we have to use the inclusion property to somehow turn this list of all possible finite sections of a qusicrystal with a rhombic window to a list of all possible finite sections of a qusicrystal with any window.

We cannot use the same method we used in the first step of this analysis since the finite sections are centered around the origin, whereas in the actual quasicrystal they may be almost arbitrarily translated.

The inclusion property only tells us that there can be no more points in the finite sections of the quasicrystal with any window inscribed to a rhombic window than in the finite sections of the quasicrystal with the rhombic window.

Naive approach to solving this would be to treat each point in each finite section of the quasicrystal with the rhombic window as optional and create a superset exhausting all options. Such superset would contain all finite sections of the quasicrystal with any window inscribed to the rhombic window, which of course includes the window we are interested in. While this is true in theory, it is very impractical for actually acquiring the list of finite sections since such superset would be enormous.

There again are many ways of solving this issue and we present the method that worked best for us. Our method slightly deviates from the course of our general quasicrystal analysis in that it does not generate a superset of all finite sections spanning $B(2\hat{R}_C)$ but rather a superset of all domains of Voronoi tiles that appear in the qusicrystal with the window we are interested in, that might but also might not be the same thing.

Just as in the previous step we are going to use a possibly incomplete list of Voronoi tiles $\{V_1, \ldots, V_m\}$, with domains $D_i = \{q_{i,1}, \ldots, q_{i,k_i}\}$, acquired by searching the Voronoi diagram of a finite section of the quasicrystal, that cover the window Ω by its intersections:

$$\Omega = \bigcup_{i \in \hat{m}} \bigcap_{j \in \hat{k}_i} (\Omega - q^*_{i,j}) \cap \Omega$$

Now assume a Voronoi tile V with domain $D = \{q_1, \ldots, q_k\}$ that appears in the quasicrystal but is missing from the list $\{V_1, \ldots, V_m\}$. Its intersection $\bigcap_{j \in \hat{k}} (\Omega - q^*_j) \cap \Omega$ has to overlap with at least one intersection of a Voronoi tile on the list, let us denote this Voronoi tile as V_p.

A point of the quasicrystal whose star map image fits both in the intersection of V and the intersection of V_p is surrounded by the points of D as well as the points of D_p. In other words the Voronoi tile V is a subset of V_p and its domain D is a subset of $D_p \cup F$, where F is a finite section of the quasicrystal with the rhombic window.

The algorithm should now be quite clear. For each $V_i \in \{V_1, \ldots, V_m\}$ and for each finite section of the quasicrystal with the rhombic window we add points of the finite section to the domain D_i and save the domain of any new Voronoi tile that is thusly created. As stated before, this creates a superset of domains of Voronoi tiles that appear in the quasicrystal.

3.2.4 Filter the superset to the final list of Voronoi tiles

This step is not at all different from what we did for the quasicrystal with one dimensional window. We follow the same three filters:

1. Eliminate duplicate Voronoi tiles.

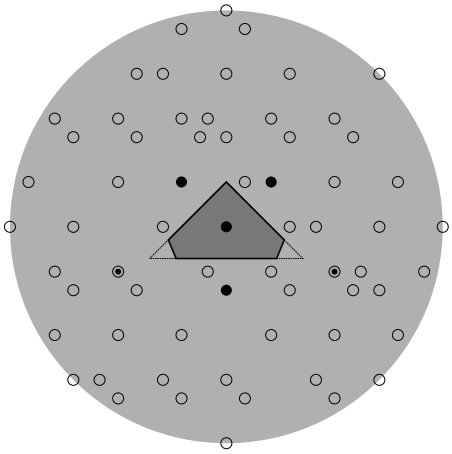

Figure 3.24: Example of how a new Voronoi tile is created from the incomplete list of Voronoi tiles and the list of finite sections. The first Voronoi tile from Figure 3.20 and the finite section from Figure 3.23 are used to create the Voronoi tile from Figure 3.22 by adding two points $\odot$ of the finite section.

2. Eliminate Voronoi tiles whose intersection $\Omega|_V = \bigcap_{i \in \hat{k}} (\Omega - q_i^*) \cap \Omega$ is empty.

3. Eliminate Voronoi tiles whose section $\Phi(V) = \Omega|_V \setminus \bigcup_{|U|<|V|} \Omega|_U$ is empty.

There might be a technical difficulty with verifying whether $\Phi(V)$ is empty. Here we again turn to the inclusion–exclusion principle we described in Section 3.1.5.

Unlike with one dimensional quasicrystals where we have picked left-closed right-open interval to avoid configurations that appear only once in the entire quasicrystal (i.e. have zero density), here we simply cannot avoid zero density configurations.

First let us explain what exactly are these zero density configurations and where do they come from. For a particular window Ω and a particular Voronoi tile V it may happen that the intersection $\Omega|_V$ is just a single point. Such Voronoi tile would appear in the quasicrystal $\Sigma(\Omega)$ only once. Additionally for the n-gonal window it may happen that a particular Voronoi tile has the intersection of a line segment. Such Voronoi tile would appear in the quasicrystal only countably infinitely many times along a line. Such Voronoi tiles are called Voronoi tiles of zero density and their domains are the zero density configurations.

Special care needs to be taken when handling these since they are present in the superset of Voronoi tiles from step 3 (Section 3.2.3) and their intersections $\Omega|_V$ technically have zero area but are not empty. We apply the filters from this step to the Voronoi tiles of zero density separately and only thereafter add the rest of them to the list of Voronoi tiles.

3.2.5 Establish the period of each Voronoi tile

Here we also use the general method described in Section 3.1.5. It differs only in the rate of growth of the area of the window, so we only illustrate the process with an example. This method however can not be used on circular windows, we deal with those separately.

Example

As an example we are going to establish a period of the Voronoi tile V with domain D from Figure 3.22 (shown again in Figure 3.25). We will assume an octagonal window Ω, such that $|\Omega| = 1$, and again we will use $\beta_8 = 1 + \sqrt{2}$ to denote the Pisot-cyclotomic number that the quasicrystal is associated to.

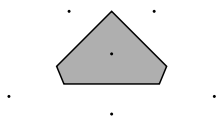

Figure 3.25: The Voronoi tile for which we establish its period.

Octagon's area increases quadratically with increased length of its edge, therefore we will assume the following formula for area of the intersection $(\omega\Omega)|_V$:

$$A = a(\omega + d)^2 \quad \text{for} \quad a, d, \omega \in \mathbb{R}$$

If we know three pairs of ω and area of the corresponding intersection, we can calculate a and d:

$$(x_1, A_1) \qquad (x_2, A_2) \qquad (x_3, A_3)$$

$$a = \frac{\frac{A_1 - A_2}{x_1 - x_2} - \frac{A_1 - A_3}{x_1 - x_3}}{x_2 - x_3} \qquad d = \frac{A_1 - A_2}{2a(x_1 - x_2)} - \frac{x_1 + x_2}{2}$$

Now to get ω_1 we calculate the area $A((\omega\Omega)|_V)$ for three different values of ω and use the formulas above:

$$x_1 = \frac{556 - 215\beta_8}{37} \qquad A_1 = \frac{163521\beta_8 - 394721}{5476}$$
$$x_2 = \frac{546 - 211\beta_8}{37} \qquad A_2 = \frac{159633\beta_8 - 385353}{5476}$$
$$x_3 = \frac{536 - 207\beta_8}{37} \qquad A_3 = \frac{155793\beta_8 - 376097}{5476}$$

$$a = \frac{1 + 3\beta_8}{2}$$
$$d = \frac{15 - 7\beta_8}{2}$$

We are looking for the area $A((\omega\Omega)|_V)$ to be zero:

$$\omega_1 + d = 0 \quad \Rightarrow \quad \omega_1 = \frac{7\beta_8 - 15}{2} \doteq 0.94975$$

Even though this method seems to be theoretically sound, we could not get reliable results for ω_2 this way. We presume that our precise arithmetic (Chapter 5) suffered from buffer overflow and thus we were not able to acquire ω_2. That however is not a deal breaker for our overall analysis.

Circular window

We could not use the approach we have just described for a circular window. Our program can do precise calculations only in $\mathbb{Q}(\beta)$ (Chapter 5) and we have not found a way to calculate an area of disc intersection in $\mathbb{Q}(\beta)$. There is however a direct way to calculate at least ω_1. Essentially we are looking for a disc radius for which the intersection $\Omega|_V$ is a single point. After some consideration we arrive to the realization that $\Omega|_V$ is a single point if the radius is half of the distance between the centers of two furthest discs. Thus we can directly calculate ω_1.

Chapter 4

Results

In this chapter we demonstrate results that can be obtained using the methods described in previous chapter.

For each Pisot-cyclotomic number we first show the number itself, several of its properties, then results of analysis of one dimensional quasicrystal.

Results for one dimensional quasicrystal entail table listing the set of distance between consecutive points of the quasicrystal for a window of certain size and two diagrams listing all possible Voronoi tiles and their periods.

For two dimensions we demonstrate our method with octagonal window and Pisot-cyclotomic number $\beta_8 = 1 + \sqrt{2}$. Due to constraints unrelated to our method (insufficient RAM), we were unable to finish the analysis for circular window and 12-fold rotational symmetry in time.

Results for the two dimensional quasicrystal were acquired following the following methodology:

1. acquire the list of Voronoi tiles for quasicrystal with window size β
2. calculate ω_1 for each Voronoi tile from the list, add each $\omega_1 \in (1, \beta]$ to list `singular`
3. acquire the list of Voronoi tiles for each quasicrystal with window size on the list `singular`
4. repeat two previous steps until the list `singular` no longer grows
5. acquire the list of Voronoi tiles for each quasicrystal with window size as mean of two consecutive values on the list `singular`

Since paper lacks convenient features such as pan and zoom we decided to not print all of the diagrams that show our results. For all diagrams we have acquired please download the package at `addurl`.

There you will find two PDFs, one showing the results for octagonal window and second showing work in progress on quasicrystals with 8-fold rotational symmetry with circular windows. Both PDFs contain division of window, list of Voronoi tiles and a finite sections of the quasicrystal for each window size.

Further we only show the lists of Voronoi tiles for the octagonal window and estimates of their periods. Since each Voronoi tile may appear in up to 16 or 24 possible orientations (rotation and reflection) we only show one representative to conserve space.

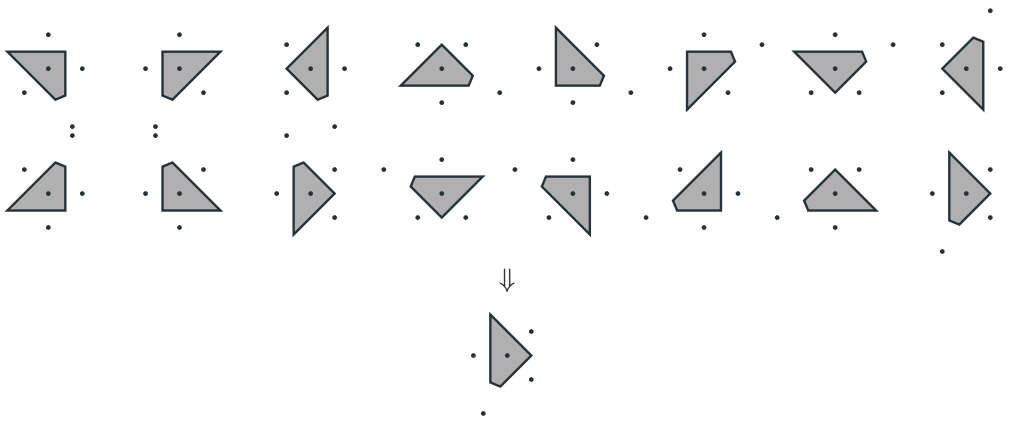

Figure 4.1: Sixteen Voronoi tiles that have the same shape and appear in various orientations are all represented by one of them.

The rows of Table 4.1 correspond to window sizes:

1. 1
2. $\frac{5\beta_8-10}{2}$
3. $5\beta_8 - 11$
4. $\frac{13\beta_8-27}{4}$
5. $\frac{3\beta_8-5}{2}$
6. $\frac{4\beta_8-5}{4}$
7. $\frac{\beta_8}{2}$
8. $\frac{3\beta_8-2}{4}$
9. $\beta_8 - 1$
10. $\frac{2\beta_8+1}{4}$
11. $\frac{3}{2}$
12. $\frac{\beta_8+4}{4}$
13. $\frac{\beta_8+1}{2}$
14. $\frac{\beta_8+5}{4}$
15. 2
16. $\frac{3\beta_8+1}{4}$
17. $\frac{3\beta_8-3}{2}$
18. $\frac{4\beta_8-1}{4}$
19. $\frac{\beta_8+2}{2}$
20. $\frac{7\beta_8-8}{4}$
21. $3\beta_8 - 5$
22. $\frac{5\beta_8-3}{4}$
23. $\frac{7-\beta_8}{2}$
24. $\frac{\beta_8+7}{4}$
25. β_8

The columns of Table 4.1 correspond to the Voronoi tiles from Figure 4.6.

4.1 One dimension: 8-fold rotational symmetry

4.1.1 Definition

$$x^2 = 2x + 1 \qquad \beta_8 = 1 + \sqrt{2} \doteq 2.414 \qquad \beta'_8 = 1 - \sqrt{2} \doteq -0.414$$

4.1.2 Formulas

$$\beta_8 \beta'_8 = -1 \qquad \beta_8 + \beta'_8 = 2 \qquad \beta_8^{k+2} = 2\beta_8^{k+1} + \beta_8^k$$

4.1.3 Distances

Remark. $\frac{1}{\beta_8} = \beta_8 - 2$

Window size	1	$(1, \beta_8 - 1)$	$\beta_8 - 1$	$(\beta_8 - 1, \beta_8)$	β_8
Distances	$\beta_8 + 1$	$\beta_8 + 1$			
	β_8	β_8	β_8	β_8	
				$\beta_8 - 1$	$\beta_8 - 1$
		1	1	1	1

4.1.4 Voronoi tiles and their periods

Figure 4.2 shows division of all windows by different Voronoi tiles and Figure 4.3 shows corresponding Voronoi tiles for selected window sizes. The period can be read from Figure 4.3 by looking up in which list does the tile first appear and then in which it disappears.

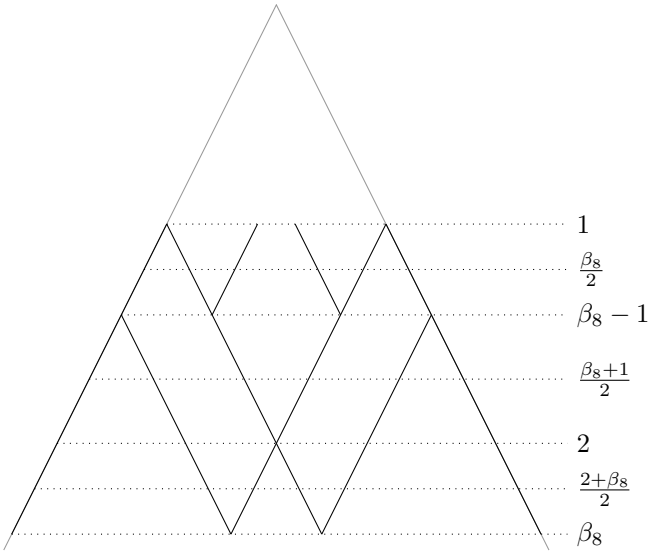

Figure 4.2: Division of window into sections corresponding to different Voronoi tiles. Each vertical slice of the trapezoid represents a single window of size in $[\beta_8 - 2, 1]$. The diagonal lines divide each window into the sections corresponding to different Voronoi tiles.

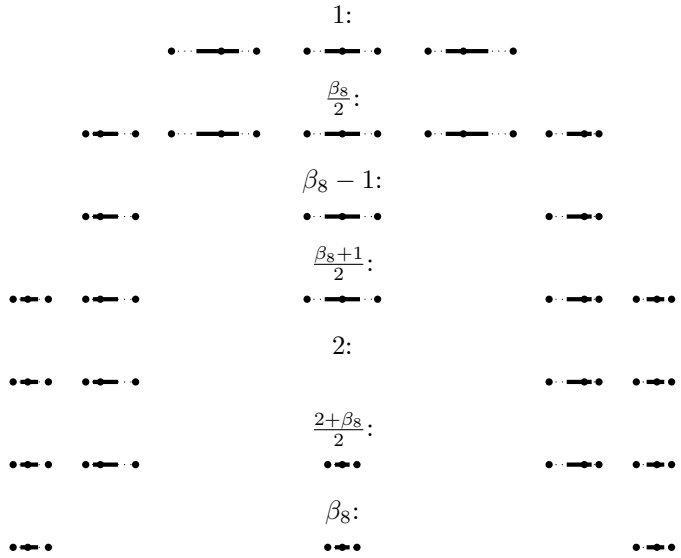

Figure 4.3: List of Voronoi tiles corresponding to sections of various windows.

4.2 One dimension: 12-fold rotational symmetry

4.2.1 Definition

$$x^2 = 4x - 1 \qquad \beta_{12} = 2 + \sqrt{3} \doteq 3.732 \qquad \beta'_{12} = 2 - \sqrt{3} \doteq 0.268$$

4.2.2 Formulas

$$\beta_{12}\beta'_{12} = 1 \qquad \beta_{12} + \beta'_{12} = 4 \qquad \beta_{12}^{k+2} = 4\beta_{12}^{k+1} - \beta_{12}^{k}$$

4.2.3 Distances

Remark. $\frac{1}{\beta_{12}} = 4 - \beta_{12}$, $\frac{\beta_{12}-2}{\beta_{12}} = 2\beta_{12} - 7$, $\frac{\beta_{12}-1}{\beta_{12}} = \beta_{12} - 3$

Window size	1	$(1, \beta_{12}-2)$	$\beta_{12}-2$	$(\beta_{12}-2, \beta_{12}-1)$	$\beta_{12}-1$	$(\beta_{12}-1, \beta_{12})$	β_{12}
Distances	β_{12}	β_{12}					
	$\beta_{12}-1$	$\beta_{12}-1$	$\beta_{12}-1$	$\beta_{12}-1$			
				$\beta_{12}-2$	$\beta_{12}-2$	$\beta_{12}-2$	
		1	1	1	1	1	1
						$\beta_{12}-3$	$\beta_{12}-3$

4.2.4 Voronoi tiles and their periods

Figure 4.4 shows division of all windows by different Voronoi tiles and Figure 4.5 shows corresponding Voronoi tiles for selected window sizes. The period can be read from Figure 4.5 by looking up in which list does the tile first appear and then in which it disappears.

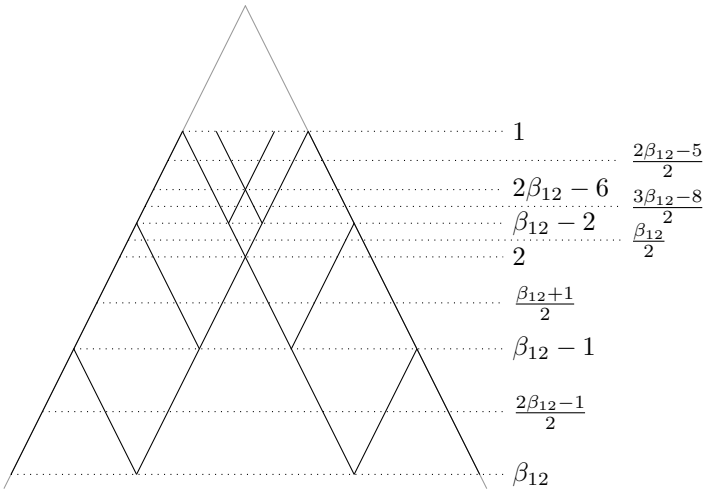

Figure 4.4: Division of window into sections corresponding to different Voronoi tiles. Each vertical slice of the trapezoid represents a single window of size in $[\beta_8 - 2, 1]$. The diagonal lines divide each window into the sections corresponding to different Voronoi tiles.

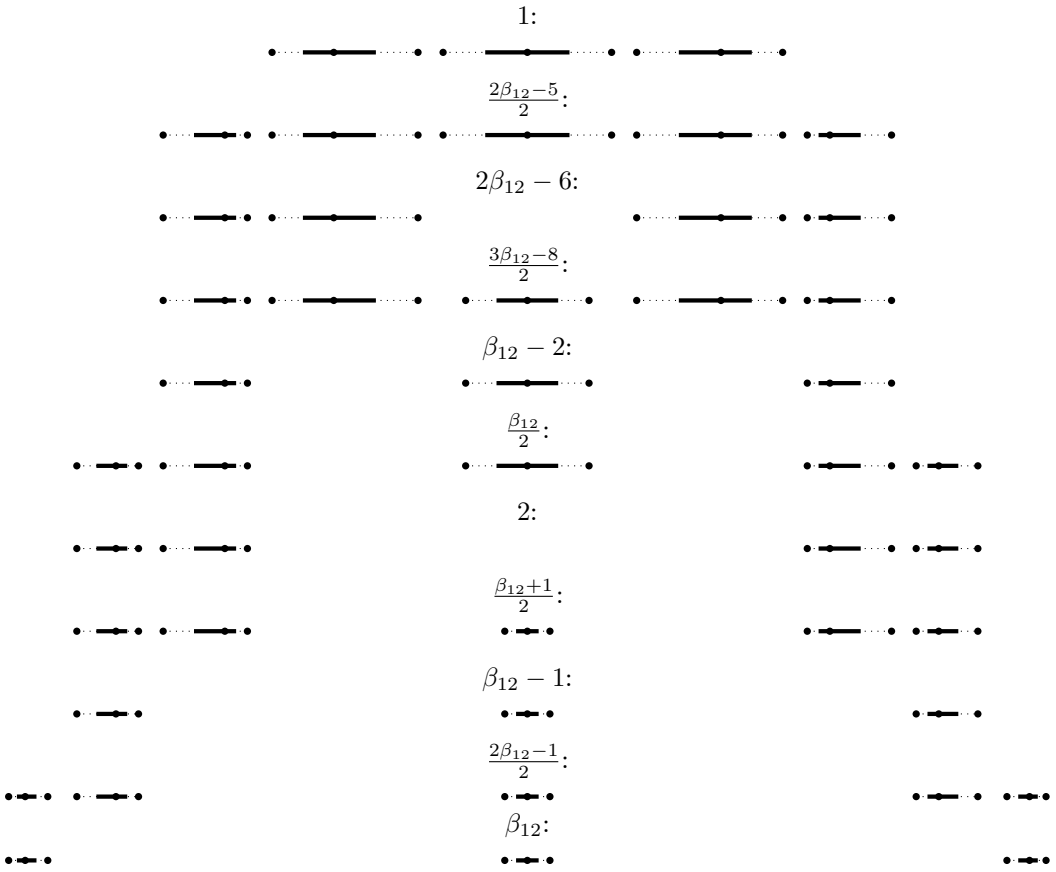

Figure 4.5: List of Voronoi tiles corresponding to sections of various windows.

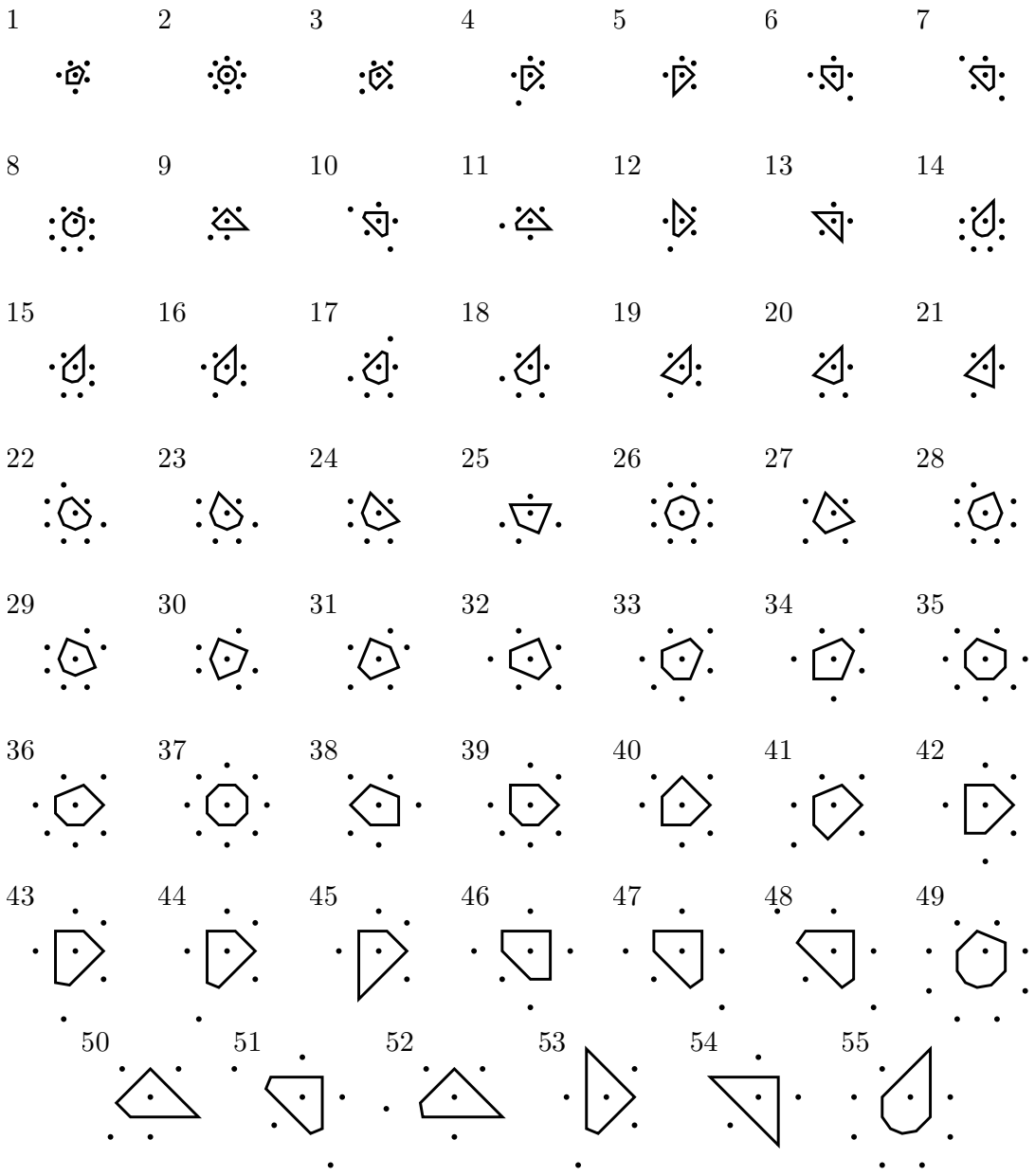

Figure 4.6: List of Voronoi tiles form quasicrystals with octagonal window.

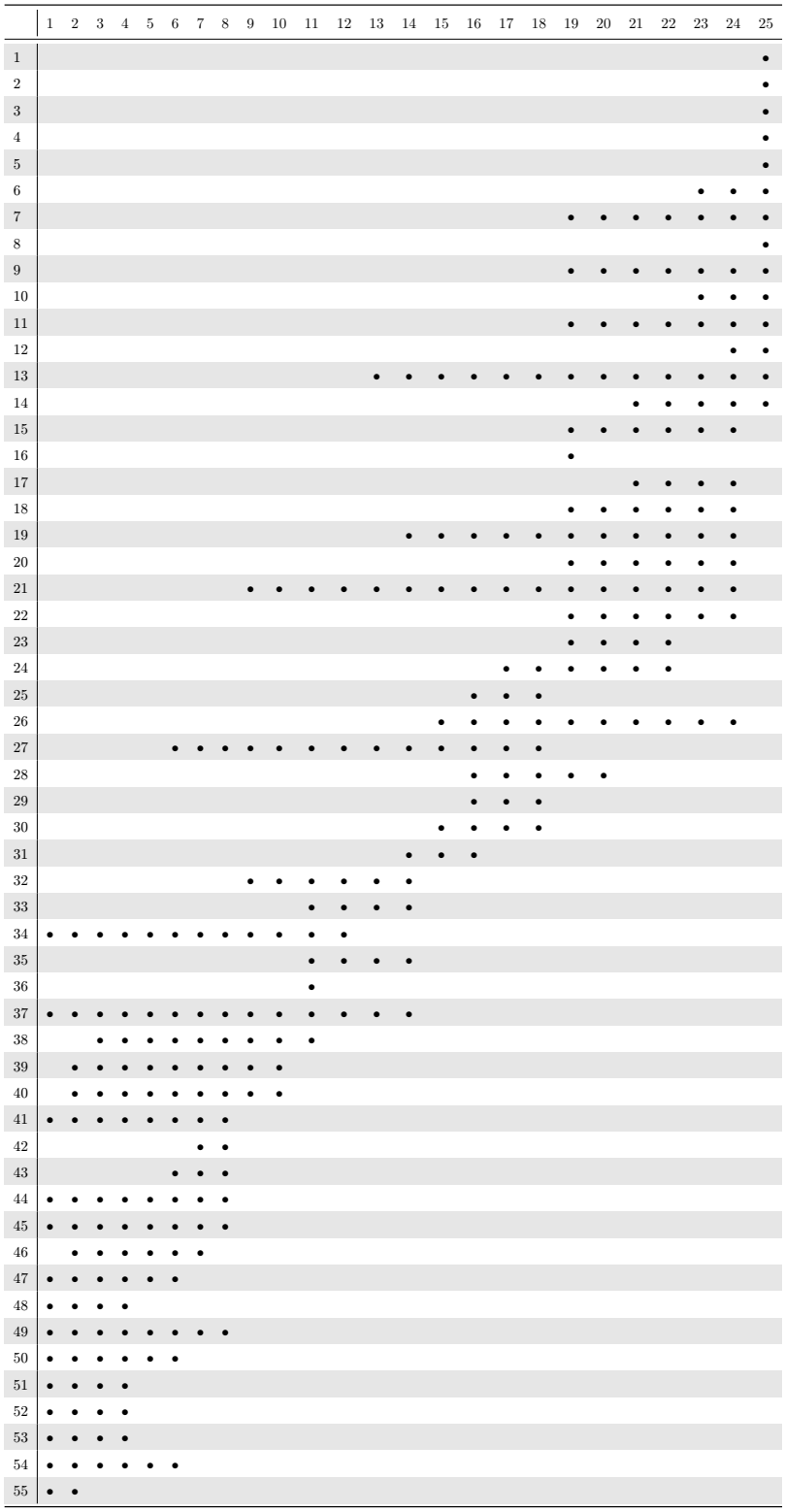

	1	2	3	4	5	6	7	8	9	10	11	12	13	14	15	16	17	18	19	20	21	22	23	24	25
1																									•
2																									•
3																									•
4																									•
5																									•
6																							•	•	•
7																			•	•	•	•	•	•	•
8																									•
9																			•	•	•	•	•	•	•
10																							•	•	•
11																			•	•	•	•	•	•	•
12																								•	•
13													•	•	•	•	•	•	•	•	•	•	•	•	•
14																					•	•	•	•	•
15																			•	•	•	•	•	•	
16																			•						
17																					•	•	•	•	
18																			•	•	•	•	•	•	
19														•	•	•	•	•	•	•	•	•	•	•	
20																			•	•	•	•	•	•	
21									•	•	•	•	•	•	•	•	•	•	•	•	•	•	•	•	
22																			•	•	•	•	•	•	
23																			•	•	•	•			
24																	•	•	•	•	•	•			
25																•	•	•							
26															•	•	•	•	•	•	•	•	•	•	
27						•	•	•	•	•	•	•	•	•	•	•	•	•							
28																•	•	•	•	•					
29																•	•	•							
30															•	•	•	•							
31														•	•	•									
32									•	•	•	•	•	•											
33											•	•	•	•											
34	•	•	•	•	•	•	•	•	•	•	•	•													
35											•	•	•	•											
36											•														
37	•	•	•	•	•	•	•	•	•	•	•	•	•	•											
38			•	•	•	•	•	•	•	•	•														
39		•	•	•	•	•	•	•	•	•															
40		•	•	•	•	•	•	•	•	•															
41	•	•	•	•	•	•	•	•																	
42							•	•																	
43						•	•	•																	
44	•	•	•	•	•	•	•	•																	
45	•	•	•	•	•	•	•	•																	
46		•	•	•	•	•	•																		
47	•	•	•	•	•	•																			
48	•	•	•	•																					
49	•	•	•	•	•	•	•	•																	
50	•	•	•	•	•	•																			
51	•	•	•	•																					
52	•	•	•	•																					
53	•	•	•	•																					
54	•	•	•	•	•	•																			
55	•	•																							

Table 4.1: Assignment of Voronoi tiles to their quasicrystals with octagonal window.

Chapter 5

Computation

It is hopefully not at all surprising that we have not made all the necessary calculations by hand, instead we have used a computer. We will not delve into the code here since it is literal transcription of the methods and algorithms we have described, just with many more lines. There however is one key tool that made it all possible: precise arithmetic in $\mathbb{Q}(\beta)$.

It is possible to implement a custom number type that does calculations precisely in field $\mathbb{Q}(\beta)$ without rounding errors. Since we have only used quadratic β, the field $\mathbb{Q}(\beta)$ has the following simple form:

$$\mathbb{Q}(\beta) = \left\{ \frac{a + b\beta}{c} \middle| a, b, c \in \mathbb{Z} \right\}$$

In other words we can represent $x \in \mathbb{Q}(\beta)$ with just three integers and since integer arithmetic is precise then even $\mathbb{Q}(\beta)$ arithmetic is precise.

Equipped with this key tool we have implemented objects for points, point sets, Voronoi tiles, windows and others with necessary properties and methods. All together we were then able to literally transcribe all the formulas and algorithms from our method of analysis.

The code is available online, but it is a result of three years of rapid prototyping, so enter at your own risk.

`https://github.com/edasubert/quasicrystal`

Conclusions

As mentioned in the introduction, this work is a successor to previous articles done by our colleges that focused on the analysis of quasicrystals with 10-fold rotational symmetry. Our method is largely based on these articles. However since the computational complexity of analysis of quasicrystals with 12-fold rotational symmetries is much higher, we could not use their method as is.

The improved covering radius estimate proved itself to be the key for progress in the analysis. In fact it seems to be so significant improvement that we could simplify the steps of analysis and thus decrease the amount of theoretical background necessary.

Although we are fairly happy with the overall size of our contribution there certainly is still a lot of work left to do.

Bibliography

[1] *The Nobel Prize in Chemistry 2011 - Popular Information.* Nobelprize.org. Nobel Media AB 2014. Web. 3 May 2017. `http://www.nobelprize.org/nobel_prizes/chemistry/laureates/2011/popular.html`

[2] E. W. WEISSTEIN. *Crystallography Restriction.* From MathWorld–A Wolfram Web Resource. `http://mathworld.wolfram.com/CrystallographyRestriction.html`

[3] J C LAGARIAS. *Geometric Models for Quasicrystals I. Delone Sets of Finite Type.* Discrete & Computational Geometry 21.2 (1999): 161-91. Web.

[4] Z MASÁKOVÁ, E PELANTOVÁ. *Teorie čísel.* V Praze: České vysoké učení technické v Praze, 2017. 178 stran. ISBN 978-80-01-06030-8.

[5] Z MASÁKOVÁ, J PATERA, E PELANTOVÁ. *Lattice-like properties of quasicrystal models with quadratic irrationalities*, Proceedings of Quantum Theory and Symmetries, Goslar, 1999, Eds. H.D. Doebner, V.K. Dobrev, J.D. Hennig, W. Luecke, World Scientific, 2000, pp. 499-509.

[6] Z MASÁKOVÁ, J PATERA, J ZICH. *Classification of Voronoi and Delone tiles in quasicrystals: I. General method.* J. Phys. A **36** (2003), 1869–1894.

[7] Z MASÁKOVÁ, J PATERA, J ZICH. *Classification of Voronoi and Delone tiles of quasicrystals: II. Circular acceptance window of arbitrary size.* J. Phys. A **36** (2003), 1895–1912.

[8] Z MASÁKOVÁ, J PATERA, J ZICH. *Classification of Voronoi and Delone tiles of quasicrystals: III. Decagonal acceptance window of any size.* J. Phys. A **38** (2005), 1947–1960.

[9] L-S GUIMOND, Z MASÁKOVÁ, E PELANTOVÁ. *Combinatorial properties of infinite words associated with cut-and-project sequences.* J. Théor. Nombres Bordeaux **15** (2003), 697–725.

[10] J ZICH. *Voronoi & Delone tiling of quasicrystals.* Fakulta jaderná a fyzikálně inženýrská České vysoké učení technické v Praze, 2002. Diplomová práce. Vedoucí práce Z Masáková.

Mentions

[11] P. H. CHEN, K. AVCHACHOV, K. NORDLUND, K. PUSSI. *Molecular dynamics simulation of radiation damage in CaCd6 quasicrystal cubic approximant up to 10 keV.* Journal of Chemical Physics, 138(23), 2013.

[12] S. DELOUDI, W. STEURER. *Higher-dimensional crystallography of N-fold quasiperiodic tilings*. Acta Crystallographica Section A, 68(2):266–277, 2012.

[13] S. KATRYCH, TH. WEBER, A. KOBAS, L. MASSUEGER, L. PALATINUS, G. CHAPUIS, W. STEURER. *New stable decagonal quasicrystal in the system Al-Ir-Os*. Journal of Alloys and Compounds, 428(1-2):164–172, 2007.

[14] D. LOGVINOVICH, A. SIMONOV, W. STEURER. *Structure of decagonal Al-Ni-Rh*. Acta Crystallographica Section B, 70(4):732–742, 2014.